UNIVERSIDADE FEDERAL DE SÃO CARLOS
PRÓ-REITORIA DE PÓS-GRADUAÇÃO E PESQUISA
PROGRAMA DE PÓS-GRADUAÇÃO EM BIOTECNOLOGIA

Análise da expressão gênica durante o reparo ósseo em defeitos de tíbias irradiados com laser *terapêutico de baixa intensidade*

Carla Roberta Tim

São Carlos
2015

Carla Roberta Tim

Análise da expressão gênica durante o reparo ósseo em defeitos de tíbias irradiados com laser *terapêutico de baixa intensidade.*

Tese de Doutorado apresentada ao Programa de Pós-Graduação em Biotecnologia da Universidade Federal de São Carlos, como parte dos requisitos para obtenção do título de Doutor em Biotecnologia

Orientadores: Prof.Dr. Ana Cláudia Rennó
Prof.Dr. Nivaldo Antonio Parizotto

São Carlos
2015

Ficha catalográfica elaborada pelo DePT da Biblioteca Comunitária/UFSCar

T582ae

Tim, Carla Roberta.
Análise da expressão gênica durante o reparo ósseo em defeitos de tíbias irradiados com laser terapêutico de baixa intensidade / Carla Roberta Tim. -- São Carlos : UFSCar, 2015.
94 f.

Tese (Doutorado) -- Universidade Federal de São Carlos, 2015.

1. Biotecnologia. 2. Reparo ósseo. 3. Laserterapia. 4. Terapia a laser de baixa intensidade. 5. Expressão gênica. I. Título.

CDD: 660.6 (20ª)

UNIVERSIDADE FEDERAL DE SÃO CARLOS

Centro de Ciências Exatas e de Tecnologia
Programa de Pós-Graduação em Biotecnologia

Folha de Aprovação

Assinaturas dos membros da comissão examinadora que avaliou e aprovou a Defesa de Tese de Doutorado da candidata Carla Roberta Tim, realizada em 27/02/2015:

Profa. Dra. Ana Claudia Muniz Renno
UNIFESP

Profa. Dra. Cristina Kurachi
UFSCar

Prof. Dr. Clóvis Wesley Oliveira de Souza
UFSCar

Profa. Dra. Mariza Akemi Matsumoto
USC

Prof. Dr. Luciana Almeida Lopes
UFSCar

DEDICATÓRIA

À minha mãe Sirlene, exemplo de honestidade, humildade e dedicação a família.
Aos meus irmãos Silmara e Marcelo,cunhados Milene e Márcio por todo esforço, carinho e apoio a mim depositado.

Amo muito todos vocês.

AGRADECIMENTOS ESPECIAIS

Com carinho a minha orientadora Profª. Drª. Ana Cláudia Muniz Rennó, pela oportunidade a mim dada, pelos ensinamentos, confiança e sobretudo pela amizade construída durante esse período de convivência. Agradeço por sua paciência, compreensão e incentivo constante para o meu estágio no exterior, foi muito importante pra mim. Por me colocar em contato com colaboradores que enriqueceram as nossas análises. Aprendi muito com você, principalmente a dedicação e o amor pela pesquisa.

Ao meu orientador Prof. Dr. Nivaldo Antonio Parizotto, pessoa tão admirável em sua humildade e sabedoria, que tão prontamente abriu-me as portas da ciência, mostrando-se sempre disposto em contribuir para o meu engrandecimento tanto no aspecto profissional quanto pessoal.Obrigada pelos conhecimentos compartilhados e, sobretudo pela amizade construída durante esse período de convivência.

Serei sempre grata aos dois!!!

AGRADECIMENTOS

Acima de tudo a Deus por ter me conduzido a realização desse sonho.

À minha querida e amada mãe, que possibilitou esta caminhada me guiando, apoiando, ensinando, com todo afeto e sabedoria. TE AMO.

Ao meu irmão Marcelo e sua esposa Milene, pela ajuda e pelo amor que demonstrou desde sempre.

À minha irmã Silmara e seu esposo Márcio, pelo incentivo, carinho e cumplicidade.

Aos meus lindos sobrinhos Gabriela, Felipe e Augusto (in memorian), que trazem felicidade a minha vida.

À toda minha família que sempre me apoio e esteve presente em todos os momentos.

À banca examinadora, pelas sugestões e críticas que contribuíram para maior clareza e entendimento deste trabalho.

Aos amigos Paulo Bossini e Hueliton Kido, pelo companheirismo, ajuda e sugestões na elaboração dessa tese e acima de tudo pela amizade construída durante esse período de convivência.

As minhas amigas Patty Brassolatti e Lia Mara Neves, mais conhecida como Snow, pelos almoços, risadas, companheirismo e acima de tudo amizade.

As amigas que conquistei no laboratório Kelly, Natália Rodrigues obrigada pelo apoio e incentivo.

Aos amigos amiga Lívia e Thiago por me acolher sempre em sua casa, pelo apoio e pelas baladas e cervejas.

As irmãzinhas de coração Vivian e Mirian Cury, pelo incentivo e acima de tudo pela amizade.

Aos queridos amigos Davilene Gigo Benato e Thiago Russo pelos ensinamentos, incentivo constante, apoio, conversas, risadas e sobretudo pela amizade ao longo desses anos.

Aos meus amigos e colegas de laboratório, Paulo Armelin, Albaíza, Tatmatsu, Daiana, Ana Laura, Vanessa, Fernanda, Toninho, Ângela, Carol, Patricia pela ajuda, estima e pelos bons momentos compartilhados.

Aos Prof. Dr. Iran Malavazzi e Anderson Cunha do Departamento de Bioctenologia pela ajuda e e seus ensinamentos.

Ao Prof. Dr. Jeroen Van den Beucken da Universidade Radbous Nijmegen - Holanda, pela oportunidade e ensinamento durante meu estágio no exterior.

Aos amigos que fiz na Holanda durante meu estágio no exterior, Simone, Antonio, Giuliana, Pedro, Paula, Alexey, Eva, XZ, Jie, Jing pela amizade e companhia durante esta fase da minha vida.

À todos os meus amigos de Fernandópolis e a todos com quem dividi uma balada e uma cerveja no final de semana.

À secretaria do programa de Biotec Claudia, pela ajuda e amizade.

Aos professores e funcionários do Departamento de Fisioterapia da UFSCar, pela atenção e ajuda.

Aos funcionários do Biotério Central da UFSCar, Roberto e Rivair pela atenção e ajuda.

Ao Laboratório Nacional de Biociência por disponibilizar o uso do software Ingenuity.

À Coordenação de Aperfeiçoamento de Pessoal de Nível Superior (CAPES) pela bolsa de estágio no exterior concedida.

Em especial, à Fundação de Amparo a Pesquisa do Estado de São Paulo (FAPESP) pelo bolsa concedida (2010-15335-0).

A todas as pessoas que contribuíram direta ou indiretamente para a realização deste trabalho.

Muito Obrigado!!!

RESUMO

Este trabalho teve como objetivo verificar os efeitos da terapia laser de baixa intensidade (LLLT) na expressão de genes relacionados à regeneração óssea de defeitos tibiais em ratos. Para isso, 100 ratos machos Wistar (3 meses de idade ± 250 gramas) foram submetidos a defeitos tibiais bilaterais e distribuídos aleatoriamente em 2 grupos experimentais (n=50). No primeiro estudo, foram avaliados os efeitos da LLLT na expressão de genes inflamatórios e angiogênicos no reparo ósseo de ratos, a partir de três grupos experimentais: grupo controle com defeito ósseo e sem tratamento (GC); grupo defeito ósseo tratado com laser 830 nm (GL). Os animais foram submetidos a irradiação laser em um único ponto sobre o defeito ósseo por 2, 3 e 7 sessões de tratamento, a cada 24 horas. A eutanásia dos animais aconteceu em diferentes períodos (36 horas, 3 dias e 7 dias após a cirurgia). A análise histológica revelou que a LLLT foi capaz de modular o processo inflamatório e induzir a deposição de tecido de granulação e osso recém formado na região do defeito ósseo. A análise com *microarray* demonstrou que a LLLT estimulou a expressão de genes relacionados com o processo inflamatório (MMD, PTGIR, PTGS2, Ptger2, IL1, 1IL6, IL8, IL18) e genes angiogênicos (FGF14, FGF2, ANGPT2, ANGPT4 e PDGFD) após 36 horas e 3 dias, seguido pela a diminuição da expressão gênica no 7° dia. A análise imunohistoquímica revelou que os animais tratados apresentaram maior imunoexpressão de COX-2 após 36 horas e aumentou a imunoexpressão de VEGF após 3 e 7 dias. Assim, os achados indicam que a LLLT foi eficiente em acelerar a deposição de tecido ósseo neoformado, provavelmente através da modulação de genes inflamatórios e angiogênicos e a imunoexpressão de COX-2 e VEGF durante a fase inicial de reparo ósseo. No segundo estudo, foram avaliadas os aspectos relacionados a estimulação de células ósseas e a neoformação do tecido ósseo, a partir de cinco grupos experimentais: GC e GL. O tratamento laser iniciou-se imediatamente após a cirurgia dos defeitos ósseos e realizaram-se 1, 2, 3, 5 e 7 sessões, com um intervalo de 24 horas entre elas. A eutanásia dos animais aconteceu em diferentes períodos (12 horas, 36 horas, 3 dias, 5 dias e 7 dias após a cirurgia) As análises histológica e morfométrica revelaram que o GL apresentou aumento de osso neoformado no defeito ósseo após 3, 5 e 7 dias. A análise com *microarray* evidenciou que a LLLT aumentou significantemente a expressão de TGF-β, BMP, FGF, RUNX-2 e OC que podem ter estimulado a proliferação e diferenciação dos osteobastos e consequentemente aumentado a deposição de osso neoformado. Dessa forma, pode-se concluir que a LLLT aumentou a expressão de genes osteogênicos, o que culminou na aceleração do reparo ósseo. Finalmente, podemos concluir que a LLLT foi eficaz em estimular a deposição óssea, ativando a expressão de genes inflamatórios, angiogênicos e osteogênicos e ainda, estimulando a imunoexpressão de proteínas relacionados a fase iniciais do reparo ósseo em defeitos tibiais em ratos.

Palavras-chave: reparo ósseo, terapia laser de baixa intensidade, *microarray*, expressão gênica.

ABSTRACT

This study aimed to evaluate the effects of low level laser therapy (LLLT) in the expression genes related to bone defect repair in tibia in rats. For this, one hundred male Wistar rats (3 months ± 250 g) were submitted to bilateral tibial defects and randomly distributed in two experimental groups (n=50). In the first study the effects of the LLLT in the expression of inflammatory and angiogenic genes in bone repair of rats were investigated in three groups: bone defect group (CG) and bone defect treated with laser 830nm (GL). Laser irradiation started immediately after the surgery and it was performed for two (36 h), three (3 days) or seven (7 days) sessions, with an interval of 24 hours between sessions. The application was punctual transcutaneously above the site of the injury. Rats were euthanized individually by carbon dioxide asphyxia in different set points (36 hours, 3 days and 7 days after surgery). Histopathological analysis showed that LLLT was able to modulate the inflammatory process in the area of the bone defect and to produce an earlier deposition of granulation tissue and newly formed bone. *Microarray* analysis demonstrated that LLLT produced an up-regulation of genes related to the inflammatory processes (MMD, PTGIR, PTGS2, Ptger2, IL1, 1IL6, IL8, IL18) and angiogenic genes (FGF14, FGF2, ANGPT2, ANGPT4 and PDGFD) at 36 h and 3 days, followed by a decrease of the gene expression on day 7. Immunohistochemical analysis revealed that treated animals presented a higher expression of COX-2 at 36 h after the surgery and an increased VEGF expression on days 3 and 7. Our findings indicate that LLLT was efficient on accelerating the development of newly formed bone probably by modulating the inflammatory and angiogenic gene expression and COX2 and VEGF immunoexpression during the initial phase of bone healing. In the second study, aspects related to bone cell stimulation and newly formed bone were evaluated in five groups: CG and LG. The laser treatment started immediately after the surgery to produce the bone defects and there have been 1, 2, 3, 5 e 7 sessions with an interval of 24 hours. Rats were euthanized in different set points (12 hours, 36 hours, 3 days, 5 days and 7 days after surgery). Histopathology revealed that treated animals produced increased amount of newly formed bone at the site of the injury. Also, microarray analysis evidenced that LLLT produced a significantly increase in the expression TGF-β, BMP, FGF, RUNX-2 and BMP, which could have stimulated osteoblast proliferation and differentiation, which may be related to improving the deposition of newly formed bone at the site of the injury. Thus, it is possible to concluded that LLLT improved bone healing by producing a significant increase in the expression of osteogenic genes. Finally, we concluded that LLLT was effective to stimulate newly formed bone by active expression of inflammatory, angiogenic and osteogenic genes and also stimulate immunoexpression of proteins related to the initial phases of bone healing in tibial defects in rats.

Key words: bone repair, low level laser therapy, microarray, gene expression.

LISTA DE ABREVIATURAS E SÍMBOLOS

ALP = Alkaline Phosphatase (Fosfatase Alcalina)

ANGPT = Angiopoietin (Angiopoitina)

ANOVA = Análise de Variância

ATP = Trifosfato de Adenosina

BMP = Bone Morphogenetic Protein (Proteína Morfogenética Óssea)

cDNA = Ácido desorribonucléico Complementar

cm^2 = Centímetro quadrado

COX-2 = Ciclo-Oxigenase-2

cRNA = Ácido ribonucléico Complementar

Cy3 = Cianina 3

Cy5 = Cianina 5

DNA = Ácido Desoxirribonucléico

EDTA = Ácido Etilenodiaminotetracético

FGF = Fibroblast Growth Factor (Fator de Crescimento Fibroblástico)

GC = Grupo Controle

GL = Grupo laser

IL = Interleukin (Interleucinas)

IPA = Ingenuity Pathways Analysis

J = Joule

J/cm^2 = Joule por Centímetro Quadrado

Laser = Amplificação de Luz por Emissão Estimulada de Radiação

LLLT = Low Level Laser Therapy (Terapia Laser de Baixa Intensidade)

M = Mol

MCSF = Macrophage Colony Stimulating Factor

MeV = Multi Experiment View

mg/kg = Miligrama por Quilograma de Massa Corporal

MIDAS = *Microarray* Data Analysis System

ml = Mililitro

MMD = Monocyte to macrophage differentiation-associated (Diferenciação associados de Monócitos para Macrófagos)

mRNA = Ácido ribonucleico mensageiro

MSCs = Mesenchymal Stem Cells

mW = MiliWatts

mW/cm^2 = MiliWatts por Centímetro Quadrado

PBS = Solução de Tampão Fosfato

PDGF = Platelet-derived Growth Factor (Fator de Crescimento Derivado de Plaquetas)

PDGFRA = Platelet-derived Growth Factor Receptor (Receptor Fator de Crescimento Derivado de Plaquetas)

PGE2 = Prostaglandin E2 (Prostaglandina E2)

pH = Potencial Hidrogeniônico

PTGER2 = Prostaglandin E Receptor 2

PTGIR= Prostaglandin I2 (prostacyclin) Receptor (Receptor Prostaglandina E2)

PTGS2 = Prostaglandin-endoperoxide Synthase 2

RNA = Ácido Ribonucléico

ROI = Regions of Interest

rpm = Rotação por Minuto

RPS18 = Ribosomal Protein S18 (Proteína Ribossomal 18)

RT-PCR = Quantitative Real Time Polymerase Chain Reaction (Reação em Cadeia de Polimerase em Tempo Real Quantitativa)

RUNX-2 = Runt-related Transcription Factor-2

TGF-β = Transforming Growth Factor-β (Fator de Crescimento de Transformação β)

TNF-α = Tumor Necrosis Factor- α (Fator de Necrose Tumoral α)

VEGF = Vascular Endothelial Growth Factor (Fator de Crescimento Vascular Endotelial)

μm = Micrômetro

LISTA DE FIGURAS

LISTA DE TABELAS

APRESENTAÇÃO

Esse trabalho foi estruturado na forma de artigos, sendo dividida em três partes e redigida de acordo com as normas do programa de pós-graduação em Biotecnologia.

A primeira parte é constituída de uma contextualização, objetivo e detalhamento da metodologia empregada.

A segunda parte compreende dois artigos que possuem como fundamentação a parte acima descrita. O primeiro trabalho aborda os efeitos da terapia laser de intensidade na resposta inflamatória e angiogênica no reparo ósseo de ratos, denominado " Effects of low level laser therapy on inflammatory and angiogenic gene expression during the process of bone healing: a *microarray* analysis", submetido ao periódico Journal of Biomedical Optics. O segundo artigo aborda os aspectos relacionados a estimulação de células ósseas e a neoformação do tecido ósseo, intitulado "Effects of low level laser therapy on expression of osteogenic genes during the initial stages of bone healing in rats: a *microarray* analysis", submetido ao periódico Lasers in Medical Science. Vale ressaltar que cada um dos artigos estão apresentados seguindo as normas de publicação dos referidos periódicos.

A terceira parte é composta das considerações finais, perspectivas futuras, referências bibliográficas e anexos.

SUMÁRIO

Parte I

---

1. CONTEXTUALIZAÇÃO

2. OBJETIVO

3. MATERIAIS E MÉTODOS

1. CONTEXTUALIZACÃO

O reparo ósseo constitui um processo altamente complexo, que inclui a interação de uma série de eventos biológicos, que determinam a restauração da integridade do tecido ósseo (BUCKWALTER *et al*., 2007; ORYAN *et al*, 2015). Assim, a ossificação endocondral se iniciam imediatamente após a fratura óssea, onde ocorre a destruição de matriz, morte celular, rompimento do periósteo e do endósteo. Ainda, vasos sanguíneos do tecido ósseo e dos tecidos moles adjacentes são rompidos e ocasionam extensa hemorragia, resultando na formação de um coágulo no local da lesão (GUARTNER e HIATT, 2003). O coágulo sanguíneo induz a sinalização de vários fatores de crescimento e angiogênicos, que por sua vez ativam a migração de células inflamatórias, que consequentemente infiltram no coágulo e iniciam a degradação do tecido necrosado (HING, 2004; ECKARDT *et al*, 2005; LU *et al*, 2006).

Subsequentemente, ocorre a invasão de células mesenquimais que se diferenciam em fibroblastos, condroblastos e osteoblastos. Tais células são responsáveis pela formação do tecido de granulação, calo ósseo não mineralizado e, posteriormente, pela formação do tecido ósseo (HADIARGYROU *et al*., 1998; MARSELL e EINHORN, 2011). A fase final no processo de reparo é o remodelamento, caracterizada pela remodelagem do calo ósseo, formação de tecido ósseo mineralizado, reconstrução do canal medular e restauração óssea (ORYAN *et al*., 2015).

Essa sequência de eventos requer a ação de diferentes células (fibroblastos, macrófagos, condrócitos, osteoblastos, osteoclastos) que são recrutadas para o sítio de lesão, e também, síntese ativa de genes, expressão de várias proteínas e fatores de transcrição e crescimento que controlam a produção e organização da matriz e estimulam a formação de novos vasos sanguíneos (SENA *et al*., 2005; CLAES e

WILLIE, 2007; KAYAL *et al.*, 2009). Dentre estes, podem ser destacados os genes: proteínas morfogéticas ósseas (BMPs) (KLOTING *et al*., 2005; YAOITA *et al*., 2000), fator de transformação de crescimento beta (TGF-β), RUNX-2 (do inglês "*Runt-related transcription factor 2*") (RATH *et al*., 2008), fator de crescimento derivado de plaquetas (PDGF), osteocalcina (OC) (SONG *et al*., 2006; YAOITA *et al*., 2000), fator de crescimento insulínico (IGF), fator de crescimento fibroblástico (FGF), angiopoitina (ANG) e através do fator de crescimento endotelial (VEGF) (SCHINDELER et al., 2008; TSIRIDIS *et al*., 2007).

As BMPs e o TGF-β apresentam uma ampla gama de funções celulares tais como recrutar células osteoprogenitoras para o local da lesão (CANALIS *et al*., 2003; CHEN *et al*., 2012; AGAS *et al*., 2013). Da mesma forma, o RUNX-2 é um fator de transcrição importante no processo de osteogênese durante o desenvolvimento esquelético (WOHL *et al*., 2009) e também esta associada a proliferação de osteoblastos desenvolvendo, com isso, um papel importante na formação óssea (STEIN *et al*., 2004; ZIROS *et al*., 2008). O PDGF é liberado pelas plaquetas e estimula a quimiotaxia dos macrófagos e assim como as BMPs, TGF-β and RUNX-2 estimula a diferenciação de osteoblastos (PHLILLIPS, 2005). A OC é sintetizada e secretada por osteoblastos maduros e osteócitos, sendo amplamente utilizado como marcador da atividade osteoblástica (ZHANG *et al*., 2002). A proliferação de fibroblasto e condrócitos é estimulada pelos os genes FGF, IGF, TGF-β e PDGF (SCHINDELER *et al*., 2008).

O desenvolvimento dos novos vasos sanguíneos é regulado principalmente por duas vias moleculares, a ANG e através do VEGF (TSIRIDIS *et al*., 2007). A expressão de ANG é induzida precocemente na cascata de cicatrização, o que sugere que elas promovem uma resposta vascular inicial (LEHMANN *et al*., 2005). A outra via envolvida é o VEGF, considerado um dos mais importantes fatores de crescimento

endotelial e indutor da angiogênese (HANKENSON *et al*., 2011). A presença de vasos sanguíneos fornece um nível apropriado de oxigênio e também são fonte de células osteoprogenitoras responsáveis pelo reparo ósseo (PACICCA *et al*., 2003).

Apesar do processo de reparo ósseo envolver um grande número de ações celulares e moleculares para proporcionar um estado normal de regeneração, no decorrer deste processo podem ocorrer alterações que interferem este processo tais como suprimento sanguíneo insuficiente, presença de tumor ósseo, presença de infecção, utilização de medicação anti-inflamatória entre outros fatores que irão culminar na deficiência da regeneração e consequentemente, no atraso da consolidação e até mesmo, na não união óssea (SENA *et al*., 2005; MARSELL e EINHORN, 2010).

Dentro deste contexto, há necessidade de desenvolvimento de novos tratamentos capazes de melhorar e ou acelerar o processo de reparo ósseo. Um tratamento promissor é o uso da Terapia Laser de Baixa Intensidade (LLLT) no tratamento de fraturas com deficiência na consolidação óssea (OLIVEIRA *et al*., 2009; BOSSINI *et al*., 2012) .

1.1 Terapia Laser de Baixa Intensidade

A LLLT é uma modalidade terapêutica efetiva e segura que tem demonstrado resultados positivos em muitas condições patológicas, com relatos de múltiplos efeitos clínicos, incluindo a cicatrização de tecidos moles e osso (BOSSINI *et al*., 2012; TIM *et al*., 2013; RODRIGUES et al., 2013; CHANG *et al*.,2014; PATROCÍNIO-SILVA *et al*.,2014). Seus efeitos nos tecidos biológicos podem ser explicados pela absorção da luz por moléculas fotorreceptoras localizadas nas células, chamadas cromóforos (DORTBUDAK, 2000). Uma vez absorvida, a energia fotônica é convertida em energia fotoquímica (KARU & KOLYAKOV, 2005) e isso ocorre predominantemente à nível

de interação molecular, conectadas a alterações dos parâmetros de homeostase celular (pH, concentração de Ca+2, ATP e outros), as quais acontecem minutos ou horas após a irradiação. Isto condiciona a ocorrência de possíveis mudanças na taxa de síntese de DNA e RNA, alterações na taxa de consumo de O_2 e alteração do potencial de membrana (BAXTER,1997; KARU & KOLYAKOV, 2005). Essas alterações podem estimular a taxa respiratória e a síntese de ATP (KARU, 1998). A ativação da cadeia respiratória pela irradiação gera um gradiente de próton na membrana mitocondrial que atua como um sinal iniciador para a proliferação celular. Com isso, serão geradas as respostas indiretas do laser nos tecidos. Entre essas respostas podemos destacar os efeitos anti-inflamatório, analgésico e cicatrizante (KARU & KOLYAKOV, 2005).

Em relação ao efeito cicatrizante, diversos trabalhos evidenciam que a LLLT pode estimular o metabolismo tecidual e a proliferação celular, justificando os resultados positivos da sua aplicação em processos de reparo após uma lesão (PINHEIRO *et al*., 2001, VLADIMIROV *et al*., 2004; NINOMIYA *et al*., 2007). Resultados encontrados em uma série de estudos, sugerem que a LLLT promove aumento na síntese de colágeno, aumento da proliferação e diferenciação de osteoblastos e fibroblastos, (OZAWA *et al*., 1998; VLADIMIROV *et al*., 2004; NINOMIYA *et al*., 2007), estimulação da angiogênese, maior recrutamento de macrófagos e da atividade fagocitária, o que resultará na aceleração do reparo de tecidos (ORTIZ *et al*., 2001; LIRANI-GALVÃO *et al*., 2006; BOSSINI *et al*., 2009).

Devido aos diversos efeitos estimulatórios apresentados pela LLLT, diversos autores vêm investigando a ação deste recurso no tecido ósseo, principalmente em culturas de células ósseas e em modelos experimentais de fraturas (SILVA e CAMILLI, 2006; RENNÓ *et al*., 2007; BOUVET-GERBETTAZ *et al*. 2009; FERNANDES *et al*., 2012). Em estudos *in vitro* com células osteoblásticas, a LLLT evidenciou o aumento da

proliferação e diferenciação celular através da estimulação da expressão dos genes RUNX-2 e BMP-2 (BOUVET-GERBETTAZ *et al*., 2009), e ainda, estimulou a atividade da proteína fosfatase alcalina (ALP) e da expressão do mRNA da osteopontina (STEIN *et al*., 2008).

Em 2007, Rennó *et al*., avaliaram os efeitos da LLLT em culturas de osteoblastos e demonstraram que esta terapia aumentou significativamente a proliferação celular e a atividade da ALP. Da mesma forma, Aleksic *et al*., (2010) relataram que a LLLT aumentou a proliferação de osteoblastos da linhagem MC3T3-E1 por meio da ativação da via de sinalização MAPK-ERK. Ainda, Pyo *et al*., (2012) mostraram que a LLLT induz a expressão gênica de BMP-2, osteocalcina e TGF- β1 em culturas de células osteoblásticas cultivadas 1 % de hipóxia.

Os benefícios da LLLT também são evidenciados em estudos com fraturas em modelos animais (BOSSINI *et al*., 2012; FERNANDES *et al*.,2012; SELLA *et al*., 2015). Fávaro-Pipi *et al*., (2011), usando um modelo experimental de defeito ósseo tibial, demonstraram que os animais tratados com LLLT apresentaram aumento da expressão do mRNA de BMP4, ALP e RUNX-2 e ainda, maior área de tecido ósseo neoformado. Similarmente, Da Silva *et al*. (2012), investigaram o efeito da LLLT em osteoblastos derivados da sutura mediana palatina de ratos após expansão rápida da maxila, no qual observou-se o aumento da atividade de ALP, aumento da mineralização e da expressão de mRNA de ALP, RUNX2, osteocalcina, colágeno tipo I e sialoproteína.

Em outro trabalho que investigou os efeitos da LLLT no tecido ósseo, Fernandes *et al*., (2012) observaram que esta terapia foi capaz de modular o processo inflamatório e induzir a expressão gênica de ALP, OC e RUNX-2 que pode ter contribuído para acelerar o reparo ósseo nos estágio iniciais da consolidação. Além disso, Tim *et al*.,

2013 observaram que a LLLT acelerou a deposição de tecido ósseo neoformado através da ativação de fatores osteogênicos (COX-2, RUNX-2 e BMP-9) em defeitos tibiais de ratos. Sella *et al*., (2015), investigaram os efeitos da LLLT no reparo ósseo de fratura femorais e evidenciaram que este tratamento aumentou a formação de tecido ósseo, o que é relevante para o processo de reparo de fraturas e consequentemente, pode ser indicada como uma ferramenta terapêutica adjuvante na prática clínica para o tratamento de lesões com déficit de reparo.

Dessa forma, estudos clínicos têm investigado os efeitos da LLLT no reparo ósseo em humanos. Angeletti *et al*., (2010) e Cepera *et al*., (2011) avaliaram os efeitos da LLLT após a rápida expansão do maxilar em pacientes e revelaram que a LLLT foi capaz de acelerar a reparação óssea. Chang *et al*., (2014) avaliaram a eficácia da terapia laser no tratamento de fratura de punho e concluíram que este tratamento pode aliviar a dor e ainda, estimular o processo de consolidação de fraturas ósseas em humanos.

Embora, estes resultados sobre a irradiação laser em tecido ósseo são encorajadores, grande parte dos estudos utilizaram períodos intermediários e tardios da cicatrização. Ainda, estes trabalhos não realizaram a avaliação completa do processo inflamatório, assim como não investigaram os mecanismos moleculares ativados pela LLLT, nos estágios iniciais do reparo, que determinam a resposta celular osteoblástica que posteriormente, induzem a formação do tecido ósseo.

Assim, foi levantada a hipótese de que o tratamento de defeitos ósseos com a LLLT pode acelerar o metabolismo do tecido e regular positivamente a síntese de genes relacionados com a proliferação de células osteogênicas o que culminará na aceleração do processo de reparo ósseo, proporcionando um tratamento com vantagens adicionais para uso clínico. Desta forma, a expressão gênica através da análise *microarray*s foi utilizada para analisar a expressão gênica global e investigar as vias que comandam o

processo de reparo após a LLLT. Além disso, foi utilizada a análise histologia para estudar a morfologia e morfometria da área de osso recém-formado em um modelo experimental de defeito ósseo tibial em ratos, 12 e 36 horas, 3, 5 e 7 dias.

2. OBJETIVO

Avaliar os efeitos da LLLT durante as etapas iniciais do processo de consolidação em defeitos ósseos induzidos em tíbias de ratos. Assim como, determinar a influência do tratamento com a LLLT nas alterações morfológicas e morfométricas nos estágios iniciais de reparo e avaliar a expressão de genes e proteínas envolvidas no processo de reparo inicial.

3. MATERIAIS E MÉTODOS

3.1 Animais

Foram utilizados 100 ratos machos da linhagem Wistar com três meses de idade e com peso corporal médio de 250-300 gramas no início do experimento, provenientes do biotério central da UFSCar. Os animais foram mantidos no biotério do Departamento de Fisioterapia da UFSCar, alimentados com ração comercial e água a vontade, mantidos em regime de luz (12 horas claro e 12 horas escuro) e temperatura controlada a 22 ± 2^{o} C. Este estudo experimental foi realizado de acordo com os princípios éticos de experimentação animal e foi aprovado pela Comissão de Ética em Experimentação Animal da Universidade Federal de São Carlos (010/2011) (ANEXO 1).

3.2 Modelo Experimental

O modelo usado no estudo foi baseado nos trabalhos de Barushka *et al*., (1995), Freitas *et al*., (2000) e Bossini *et al*., (2012) ao promoverem defeitos ósseos esféricos de dimensões padronizadas na cortical da tíbia de ratos, com a utilização de uma broca odontológica acionada por um micromotor.

3.3 Procedimento Cirúrgico

Para a realização dos defeitos ósseos os animais foram pesados e posteriormente anestesiados de acordo com a massa corporal, utilizando-se uma combinação a base de cloridrato de ketamina (80 mg/Kg) e cloridrato de xilazina 2% (12 mg/kg), aplicado intraperitonialmente. Após a anestesia, foi realizada a tricotomia e antisepsia da área a

ser operada, em seguida efetuada uma incisão no terço proximal da tíbia direita e esquerda (Figura 1A e 1B). A lesão foi realizada 10 mm abaixo da articulação do joelho (Figura 1C), constantemente irrigada com soro fisiologico, com a utilização de uma broca odontológica tipo trefina, da marca WMA - Brasil, com 2cm de comprimento, 3mm de diâmetro externo e acionada por um micromotor da marca BELTEC – Brasil, com rotação de 13.500 rpm, na posição horizontal e perpendicular em relação ao eixo longitudinal do osso, de modo a penetrar a cortical medial e danificar o canal medular abaixo desta, porém sem atingir a face contralateral, promovendo um orifício com 3mm de diâmetro (Figura 1D e 1E).

Em seguida, o tecido muscular e a pele foram suturados com fio de náilon monofilamentar 4.0 (Shalon®) à distância de 0,5cm entre os pontos e realizada a antissepsia local (Figura 1F). Os animais foram mantidos em caixas individuais com livre acesso à água e ração até o momento da eutanásia (TIM *et al*., 2013; BOSSINI *et al*., 2012).

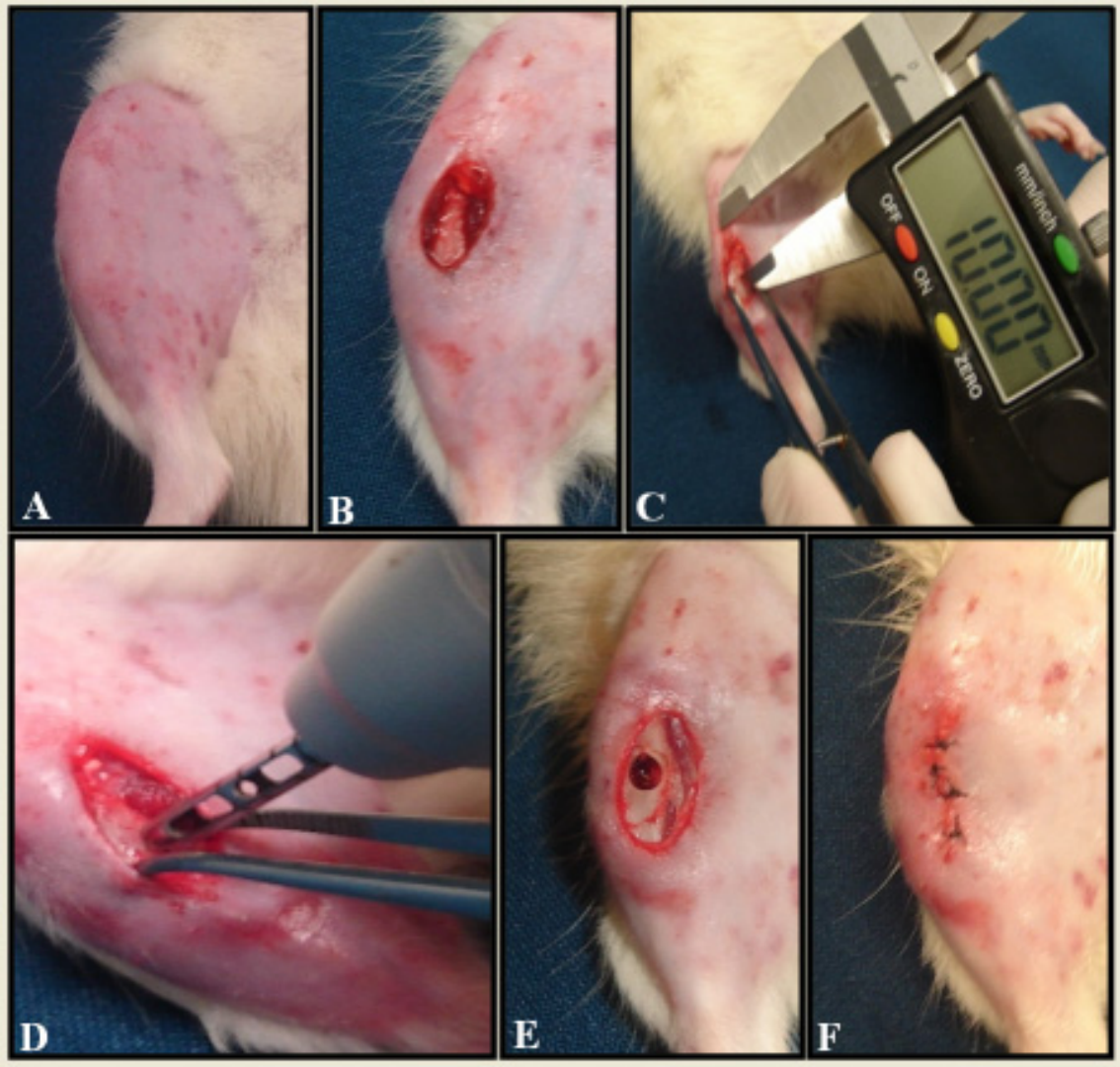

Figure 1. Procedimento cirúrgico experimental. **A:** Tricotomia da região a ser operada. **B:** Incisão da pele no terço médio tibial. **C:** Padronização com paquímetro digital. **D:** Defeito ósseo realizado com broca tipo trefina de 3mm de diâmetro. **E:** Defeito ósseo. **F:** Sutura da área operada.

3.4 Delineamento Experimental

Após os procedimentos cirúrgicos, os animais foram distribuídos aleatoriamente em dois grupos (n=50):

- ✓ **Grupo controle (GC):** animais submetidos ao defeito ósseo, mas não receberam nenhum tipo de tratamento.
- ✓ **Grupo Laser (GL):** animais submetidos ao defeito ósseo e tratados com LLLT (λ = 830nm).

Os dois grupos foram divididos em 5 subgrupos (compostos por 10 animais cada) de acordo com as datas de eutanásia no pós-operatório: subgrupo A (eutanasiado 12 horas pós-cirurgia); subgrupo B (eutanasiado 36 horas pós-cirurgia); subgrupo C (eutanasiado 3° dia pós-cirurgia); subgrupo D (eutanasiado no 5° dia pós-cirurgia) e o subgrupo E (eutanasiado no 7° dia pós-cirurgia).

3.5 Terapia Laser de Baixa Intensidade

O aparelho utilizado foi um modelo portátil de Laser (Thera Laser - DMC, São Carlos - Brasil) com comprimento de onda 830 nm, emissão contínua, potência de saída de 30 mW, diâmetro do feixe de 0,6 mm, divergência de 1.5°, na fluência de 100 J/cm^2, tempo de aplicação de 94 segundos e energia de 2.8 J, (Figura 2A). Este aparelho foi fornecido pelo Laboratório de Eletrotermofototerapia, do Departamento de Fisioterapia, da UFSCar, sob responsabilidade do Prof. Dr. Nivaldo A. Parizotto. O protocolo de tratamento com a LLLT iniciou imediatamente após o procedimento cirúrgico e foram realizados a cada 24 horas, totalizando 1, 2, 3, 5 e 7 sessões, dependendo do período experimental. Foi utilizado um único ponto de aplicação sobre o defeito ósseo, o qual foi palpado e medido com um paquímetro para padronização do local de aplicação. Nas aplicações, foi utilizada a técnica pontual em contato, sendo a caneta do equipamento posicionada perpendicularmente ao tecido e as irradiações realizadas sempre no mesmo horário (Figura 2B).

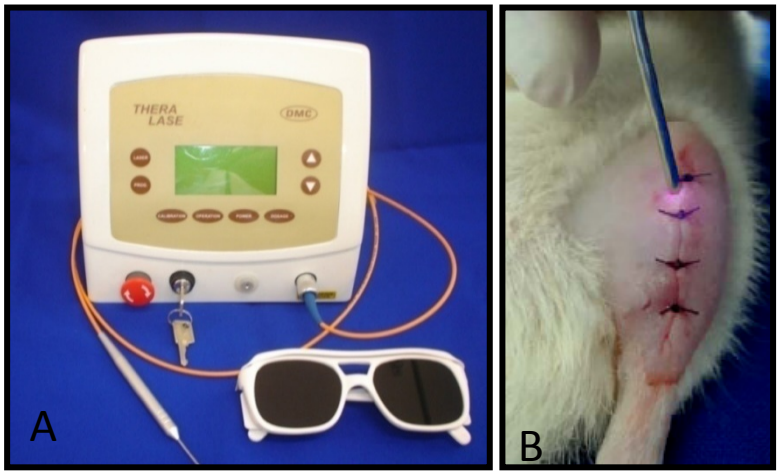

Figure 2. A: Aparelho portátil de laser utilizado no tratamento dos animais. **B:** Demonstração da área onde foi aplicada a LLLT.

3.6 Coleta e Preparação das Amostras

Os animais foram eutanasiados individualmente em câmera de CO_2 após 12 e 36 horas, 3, 5 e 7 dias. Após a eutanásia, foi realizada a ressecção cirúrgica completa das tíbias, sendo a tíbia direita designada para análise gênica e foi rapidamente congelada em nitrogênio liquido e armazenadas em freezer -80°. A tíbia esquerda foi utilizada para análise histológica e imunohistoquímica. Após dissecadas as tíbias foram fixadas em formalina tamponada a 10% por 24 horas, lavadas em água corrente por 24 horas e submetidas à descalcificação em solução de ácido etilenodiamino tetra-cético (EDTA), com trocas de 3 vezes por semana por aproximadamente 40 dias.

Depois de completada a descalcificação, as amostras foram reduzidas para processamento e para inclusão em parafina. Na sequência, os blocos de parafina foram cortados longitudinalmente, em relação ao osso, por meio de um micrótomo rotativo numérico (Leica RM—2145, Darmstadt - Germany) do Laboratório de

Eletrotermofototerapia (UFSCar), obtendo-se cortes semi-seriados com espessura 5µm e corados com Hematoxilina e Eosina (H.E.) (Merck, Darmstadt - Germany).

3.7 Análise Histopatológica Descritiva

A análise histopatológica descritiva foi realizada por dois observadores, através das lâminas coradas com H.E, considerando para cada animal a presença e intensidade dos seguintes achados histopatológicos: hematoma, processo inflamatório, fibrina, tecido de granulação, tecido ósseo neoformado e organização tecidual (FERNANDES *et al*., 2012).

3.8 Análise Morfométrica

A análise morfométrica quantitativa foi realizada nas lâminas coradas com H.E. Para a realização desta análise, foi utilizado um microscópio Nikon E 20000 e o programa de imagem Motic Imagens Plus versão 2.0 para a obtenção de fotomicrografias e análise das imagens, respectivamente. Foram selecionados 5 campos pré-determinados da região da lesão de cada lâmina: campo 1 (próximo da margem superior do defeito ósseo), campo 2 (próximo da margem direita do defeito ósseo), campo 3 (próximo da margem inferior do defeito ósseo), campo 4 (próximo da margem esquerda defeito ósseo) e campo 5 (no centro do defeito ósseo). Cada campo foi fotografado com a objetiva de 10x, e teve toda a área de neoformação óssea contornada, com o valor expresso em μm^2. Os valores das áreas de osso neoformado de cada campo foram armazenados em arquivo Excel e os valores dos cinco campos de uma mesma lâmina foram somados, revelando o valor total da área de osso neoformado para o

animal analisado (OLIVEIRA *et al*., 2009; FÀVARO-PÍPI *et al*., 2010; BOSSINI *et al*., 2012).

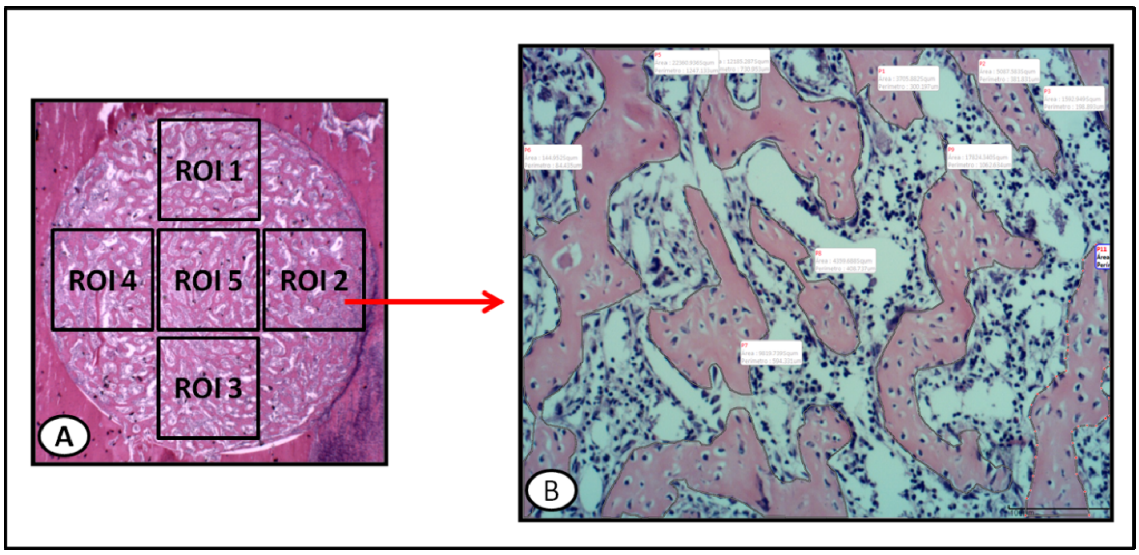

Figure 3. A: Desenho ilustrativo da padronização dos campos selecionados na análise morfométrica. **B:** Fotomicrografia representando o campo 2, com a marcação da área de neoformação óssea. Coloração H.E. (200 µm).

3.9 Análise Gênica

3.9.1 Extração de RNA

As tíbias direitas congeladas foram reduzidas 2 milímetros acima e abaixo do local do defeito ósseo e maceradas com o auxílio de um pulverizador de tecidos (D.L.MICOF, São Paulo - Brasil) previamente mantido em gelo seco por 15 minutos. O "pó" das tíbias maceradas foi transferido para um cadinho de porcelana resfriado no gelo com 1 ml de Trizol (Invitrogen, Carlsbad - Estados Unidos). Em seguida, as amostras foram homogeneizadas no homogenizador Power Gen 1000 S1 (Fisher

Scientific, Waltham - Estados Unidos) em tubos de micrografia. Na sequência, foi realizada a centrifugação das amostras a 12000 x g por 1 minuto (4°C), transferência do sobrenadante para um novo microtubo e incubação por 5 minutos em temperatura ambiente.

Transcorrido o tempo, foram adicionados 200 µl de clorofórmio para separação das diferentes frações (DNA, RNA e proteína) seguido de agitação vigorosa e incubação por 15 minutos em temperatura ambiente. Após a incubação, foi realizada a centrifugação por 15 minutos a 12000 x g (4°C) e transferência da fase aquosa superior (contendo a fração de RNA) para um novo microtubo. Por fim, foram adicionados 450 µl de isopropanol para precipitação do RNA total e o material foi incubado por 10 minutos em temperatura ambiente. As amostras foram centrifugadas por 10 minutos a 12000 x g (4°C) e os precipitados foram lavados com 1000 µl de etanol 75%. Para ressuspender o RNA total precipitado foi utilizada água livre de RNAse.

3.9.2 Purificação das Amostras

O RNA total extraído foi purificado utilizando o kit illustra RNAspin mini (General Electric, Estados Unidos). Para cada 10 µl de RNA total acrescentou-se 35 µl de tampão RA1 e 35 µl de etanol 100%, homogeneizados em vórtex e transferido para uma coluna (com membrana de sílica). Para promover a ligação do RNA a membrana de sílica foi realizada a centrifugação por 1 minuto a 8.000 x g. Em seguida, aplicou-se 350 µl de tampão MDB à coluna, seguida da adição de 90 µl de DNAse. A reação foi mantida à temperatura ambiente por 15 minutos, interrompida com a adição de 200 µl de tampão RA2 e centrifugada por 1 minuto a 11.000 x g. A coluna foi lavada com 600 µl e em seguida com 250 µl de tampão RA3. Para eluir o RNA preso à coluna,

adicionaram-se 30 µl de água livre de RNAse e centrifugou-se as amostras por 1 minuto a 11.000 x g. O RNA purificado foi separado em várias alíquotas e armazenado em freezer -80°C.

3.9.3 Quantificação e Avaliação da integridade do RNA total

A concentração do RNA purificado foi determinada por espectrofotometria, utilizando o espectrofotômetro NanoVue (General Electric, Estados Unidos).

Para a avaliação da integridade foi utilizado o Kit RNA 6000 Nano (Bioanalyzer, Agilent Technologies, Waldbronn, Germany), que se baseia na separação eletroforética do RNA em *microchips* e leitura do sinal de fluorescência no aparelho Agilent 2100 Bioanalyzer. Neste método, a integridade do RNA é determinada pelo cálculo do RIN (*RNA Integrity Number*). Este sistema visa demonstrar a qualidade do RNA e baseia-se em "notas" de 1 a 10 que são dadas às amostras, sendo que 1 corresponde ao maior grau de degradação e 10 ao maior grau de preservação do RNA.

3.9.4 Análise *Microarray*

As hibridizações de *microarray* foram realizadas com a plataforma Agilent Whole Rat Genome *Microarray* 4x44 K. As marcações e hibridizações foram realizadas usando o sistema de análise Agilent Two-Color (Agilent Technologies, USA). Resumidamente, o RNA total das amostras (1 ug) foi incubado com os controles internos do kit, na diluição adequada (RNA Spike A ou B). Após, foi realizada a síntese de cDNA, incubando-se as amostras na presença do *primer* T7 *promoter.* A desnaturação do *primer* foi realizada a 65°C por 10 minutos. Posteriormente, foi

adicionado à reação o cDNA master Mix (5X Strand Buffer, 0,1M DTT, 10mM dNTPs, MMLV-RT e RNAseOut). Esta mistura foi incubada a 40°C por 2 horas para síntese de cDNA, sendo posteriormente colocada a 70°C por 15 min. Em seguida, foi realizada a síntese de cRNA, adicionando-se as amostras o mix do fabricante (Agilent transcription master mix, contendo 4X transcription buffer, DTT 0,1 M, NTP mix, 50% PEG, RNaseOut, pirofosfatase inorgânica e T7 RNA polymerase). À esta mistura foram adicionados os marcadores Cy-3 nas amostras controle e Cy-5 nas amostras tratadas com LLLT. Para a síntese de cRNA marcado as reações foram incubadas a 40 °C por 2 horas. O cRNA marcado foi finalmente purificado utilizando o kit illustra RNAspin mini (General Electric, Estados Unidos) e quantificados através do NanoVue (General Electric, Estados Unidos).

Para a hibridização foram misturados 825 ng de cada cRNA das amostras marcadas com Cy-3 e Cy-5. À mistura foi adicionado o Agilent Fragmentation Mix (10X *Blocking Agent*, 25X *Fragmentation Buffer*), incubando-se a reação a 60°C por exatos 30 minutos, para a fragmentação do RNA. A fragmentação foi interrompida adicionando-se o tampão de hibridização (2X GE Hybridization Buffer HI-RPM). Finalmente, 100 µL de cada amostra foram colocadas nas lâminas contendo os microarranjos de oligonucleotídeos. As lâminas foram então condicionadas em forno de hibridização (Agilent G2545A Hybridization Oven) a 65°C, por 17 horas.

Após o período de hibridação, as lâminas foram lavadas com os tampões de lavagem, Wash buffer 1 (GE Healthcare) (tempo livre a temperatura ambiente), Wash buffer 1 (GE Healthcare) (1 minuto a temperatura ambiente) Wash buffer 2 GE (1 minuto a 37°C), Acetonitrila (Sigma-Aldrich) (10 segundos a temperatura ambiente), *Stabilization and Drying* (Agilent Technologies, Waldbronn, Germany) (30 segundos a

temperatura ambiente) e escaneadas com o aparelho GenePix 4000B *microarray* scanner (Molecular Devices, USA).

3.9.5 Análise das imagens e dados obtidos do *Microarray*

As imagens geradas através do escaneamento das lâminas de *microarray* foram analisadas utilizando-se o software Agilent Feature Extraction (FE), versão 11.5 (Agilent Technologies, USA), que faz uso do algorítmo de normalização por Lowess, obtendo-se a subtração do *background* e a normalização dos valores de intensidade da fluorescência de Cy-3 e Cy-5. Os dados normalizados pelo FE foram convertidos em novo formato de arquivo utilizando-se o software Express Converter (versão 2.1, TM4 available at http://www.tm4.org/utilities.html), que converte os arquivos Agilent em arquivo com extensão MeV (multi experiment view), arquivos esses compatíveis com a plataforma TM4 para análise de expressão gênica. Os novos arquivos, uma vez com extensão .MeV, foram carregados no software MIDAS (TM4 platform), onde foi calculada a média dos dados obtidos de genes replicados em cada *microarray*, a partir das triplicatas biológicas de cada período experimental. Finalmente, os dados completamente normalizados foram analisados através do software TIGR MeV (TM4 platform, Multi Experiment Viewer, disponível em http://www.tigr.org/software/*microarray*.shtml), por meio do qual os genes diferencialmente expressos foram estatisticamente considerados significantes quando a razão do $\log_2$ da expressão (Cy3/Cy5) foi diferente de zero, o que indica a ausência de modulação da expressão gênica.

3.9.6 Análise Funcional utilizando o programa Ingenuity Pathways Analysis (IPA).

Ingenuity Pathways Analysis versão 4.0 (Ingenuity Systems, Mountain View, CA, EUA) foi utilizado para pesquisar possíveis vias e redes biológicos. Ao comparar os dados de *Microarray*, a lista de genes foi transformada em um conjunto de redes e vias canônicas de genes relevantes. Em seguida, foi construída uma rede global hipotética, mostrando as conexões gênicas mais relevantes, diretas e indiretas, regulados pela LLLT.

3.9.7 PCR em Tempo Real

O PCR em tempo real foi realizado para confirmar os resultados obtidos pela análise *Microarray*. O RNA total foi extraído e purificado utilizando os protocolos experimentais descritos acima. O DNA complementar (cDNA) foi sintetizado a partir do RNA total extraído (1,0 µg), utilizando High-capacity cDNA Reverse Transcription (Life Technologies, Carlsbad, USA), seguindo normas do fabricante. O cDNa foi submetido a PCR em tempo real quantitativo utilizando o termociclador Applied Biosystems StepOneTM Real-Time PCR System (Life Technologies, Carlsbad, USA). A reação de PCR em tempo real foi padronizada para os *primers* RPS18, PTGER2, IL1, ANG4, PDGFD e FGF2. A programação consistiu de uma desnaturação inicial 94 °C por 10 minutos, seguido de 40 ciclos com desnaturação a 94 °C por 15 segundos, anelamento a 60 °C por 1 minuto e extensão a 72 °C por 45 segundos. Controles negativos foram incluídos em cada corrida, em que a amostra era substituída por água deionizada. Cada gene foi amplificado simultaneamente em duplicata. A análise de

expressão gênica relativa foi realizada utilizando o método $2^{-\Delta\Delta CT}$. O gene RPS18 foi utilizado como constitutivo para normalizar os dados de expressão.

Tabela 1. Sequências de *primers* utilizados nos experimentos de PCR em tempo real.

Gene	*Forward primer*	*Reverse primer*
RPS18	GTGATCCCCGAGAAGTTTCA	AATGGCAGTGATAGCGAAGG
PTGER2	GAACTGCGAGAGTCGTCAGTATCTC	CCCCGGCCGTGAACAT
IL1	AAGTGGAATGGGTCGGAAATT	TGAAGGGTGTTCCAAAAACTGA
ANGPT4	GGCATCTACTATCCGGTTCATCA	CATGCGTGTGCCATGCA
PDGFD	TATGCTCATTGGATGCCTTGTC	TGCTGCTATCGGGACACTTTT
FGF2	AAGGATCCCAAGCGGCTCTA	CGGCCGTCTGGATGGA

3.10 Imunohistoquímica

Para a análise imunohistoquímica as lâminas foram imunocoradas para detectar a expressão de COX-2 e VEGF. Após a desparafinização e hidratação dos cortes foi realizado o bloqueio da peroxidase endógena, em que os mesmos foram incubados em solução a 30% de peróxido de hidrogênio. As lâminas foram incubadas com anticorpos primários nas seguintes diluições e tempos: *anti-Cyclooxygenase-2* (COX-2, Cat. n° sc-1747) policlonal anticorpo primário e *anti-vascular endothelial growth factor* (VEGF, Cat. n° sc-1881) policlonal anticorpo primário, ambos na concentração de 1:200 (Santa Cruz Biotechnology, Santa Cruz, USA). Após lavagem em PBS, foi aplicado o anticorpo secundário (ABC kit, PK-6200, Vector laboratories, Burlingame, CA, USA) na diluição 1:5 por 30 minutos. Em seguida os cortes foram novamente lavados em PBS e corados com diaminobenzidine (DAB, SK-4100, Vector laboratories, Burlingame, CA, USA) por 30 minutos. Por fim, foi realizada a coloração por hematoxilina e

montagem das lâminas. Para o controle negativo os anticorpos primários foram omitidos.

Imunomarcações de COX-2 e VEGF foram avaliadas tanto qualitativamente (presença das imunomarcação) quanto semi-quantitativamente em cinco campos pré-determinados utilizando um microscópio de luz (Leica Microsystems AG, Wetzlar, Alemanha) de acordo com uma escala de pontuação variando de 1 a 4 (1 = ausente, 2 = ligeiro 3 = moderada e 4 = intensa). A análise imunohistoquimica foi realizada por dois observadores.

3.11 Análise Estatística

Os dados foram analisados estatisticamente seguindo-se técnicas descritivas, tais como tabelas e gráficos, na forma de médias e erro padrão. Para as análises morfometricas e imunohistoquímica, comparação entre os grupos foi utilizada a análise de variância (ANOVA), Shapiro–Wilk's W. As análises foram realizadas com o auxílio do programa computacional STATISTIC version 7.0. O nível de significância estabelecido foi de 5% (valor descritivo de $p < 0,05$).

Parte II

4. Estudo 1

"Effects of low level laser therapy on inflammatory and angiogenic gene expression during the process of bone healing: a *microarray* analysis"

5. Estudo 2

"Effects of low level laser therapy on expression of osteogenic genes during the initial stages of bone healing in rats: a *microarray* analysis"

4. ESTUDO 1

Effects of low level laser therapy on inflammatory and angiogenic gene expression during the process of bone healing: a *microarray* analysis

Carla Roberta. Tim[1], Paulo Sérgio Bossini[2], Hueliton Wilian Kido[1], Iran Malavazi[3], Marcia Regina von Zeska Kress[4], Marcelo Falsarella Carazzolle[5,6], Nivaldo Antonio Parizotto[1], Ana Cláudia Rennó[2].

[1]Federal University of São Carlos, Department of Physiotherapy, Rod Washington Luis Km 235, São Carlos, Brazil, 13565-905.
[2]Federal University of São Paulo, Department of Bioscience, Av. Ana Costa 95, Santos, Brazil, 11050-240.
[3] Federal University of São Carlos, Department of Genetics and Evolution, Rod Washington Luis Km 235, São Carlos, Brazil, 13565-905.
[4] University of São Paulo, School of Pharmaceutical Sciences of Ribeirão Preto, Department of Clinical Analysis, Toxicological and Bromatological, Av. do Café 95, Ribeirão Preto, Brazil, 14049-900, Brazil
[5]State University of Campinas, Department of Genetics and Evolution, Cidade Universitária Zeferino Vaz, Campinas, Brazil, 13083-970.
[6]Brazilian National Center for Research in Energy and Materials, Brazilian Biosciences National Laboratory, Giuseppe Máximo Scolfaro 10.000, Campinas, Brazil, 13083-970.

Corresponding author
Ana Claudia Muniz Renno, Federal University of São Paulo, Department of Bioscience, Av. Ana Costa 95, Santos, Brazil, 11050-240.
Tel.: +55 13 32218058; fax: +55 13 32232592. E-mail: a.renno@unifesp.br

4.1 Abstract: We investigate the process of bone healing and the expression of inflammatory and angiogenic genes after low level laser therapy (LLLT) in an experimental model of bone defects. Sixty Wistar rats were distributed into control and laser group (830 nm, 30 mW, 2,8 J, 100 J/cm²). Histopathological analysis showed that LLLT was able to modulate the inflammatory process in the area of the bone defect and to produce an earlier deposition of granulation tissue and newly formed bone. *Microarray* analysis demonstrated that LLLT produced an up-regulation of genes related to the inflammatory process (MMD, PTGIR, PTGS2, Ptger2, IL1, 1IL6, IL8, IL18) and angiogenic genes (FGF14, FGF2, ANGPT2, ANGPT4 and PDGFD) at 36 h and 3 days, followed by the decrease of the gene expression on day 7. Immunohistochemistry analysis revealed that treated animals presented a higher expression of COX-2 at 36 h after the surgery and an increased VEGF expression on days 3 and 7. Our findings indicate that LLLT was efficient on accelerating the development of newly formed bone probably by modulating the inflammatory and angiogenic gene expression and COX2 and VEGF immunoexpression during the initial phase of bone healing.

Key words: bone repair, LLLT, *microarray*, gene expression.

4.2 INTRODUCTION

Fracture healing is a multistage repair process that involves complex and well-orchestrated steps that are initiated in response to the injury, with the purpose of recovering bone mechanical function.[1,2] In general, bone tissue has the ability of healing by itself.[7] However, under critical conditions as for example, in larger bone defects and fractures with inadequate or interrupted vascularization, a delay in the process of healing or even a nonunion can happen.[8] Thereby, innovative clinical approaches have been developed in order to stimulate bone healing including low-level laser therapy (LLLT).[9,10]

LLLT irradiation stimulates mitochondrial metabolism, resulting in an increased expression of adenosine triphosphate (ATP), molecular oxygen production[11] and transcription factors.[12] These effects can increase the synthesis of DNA, RNA and cell-cycle regulatory proteins, therefore stimulating cell proliferation.[13-14] Moreover, LLLT could be modulate of expression of some inflammatory mediators such as interleukin 1β, (IL1β), interleukin 6 (IL6), interleukin 10 (IL10) and tumor necrosis factor α (TNFα).[15-18] Furthermore, it has been demonstrated that LLLT can stimulate angiogenesis, which is an essential part of the healing process.[19,20]

Based on the effects of LLLT cited above, this therapeutic modality has been used to promote wound healing, to accelerate tissue repair and to modulate the inflammatory process after injuries.[21,22] Furthermore, the effects of LLLT on the process of bone consolidation have been demonstrated, showing an increased osteoblastic activity[23], neoangiogenesis and a higher newly formed bone deposition at the site of the fracture.[21,22] In a recent *in vivo* study, Bossini *et al.*[19] observed that LLLT (830 nm) was

able of increasing newly formed bone and angiogenesis at the site of the fracture in an experimental model of bone defect in the tibias of rats.

Although the encouraging data concerning the osteogenic potential of LLLT, the molecular and cellular mechanisms by which this therapy acts on tissues remain unclear. [24,25] Moreover, there is a lack of works in the literature describing the effects of LLLT in expression of inflammatory and angiogenic genes in early fracture healing. Thus, with the advent of more sophisticated techniques in gene expression analysis (i.e. *microarray*s), it has become possible to examine the global gene expression and to investigate entire pathways that commands biological processes. Thereby, *microarray* can be very helpful in identifying possible genes regulated by LLLT during the process of bone healing.[26]

In view of the aforementioned information, it was hypothesized that LLLT can regulate the expression of genes involved in the inflammatory process and angiogenesis, which may accelerate the process of bone repair. Consequently, the present study aimed to investigate the histological modifications in the bone callus and to study the expression of genes related to the inflammatory process and the formation of new blood vessels after LLLT irradiation in the initial stages of healing.

4.3 MATERIALS AND METHODS

4. 3.1 Experimental design

Sixty male wistar rats (aged 12 weeks; weight ~300 g) were used in this study. This study was conducted in accordance with the Guide for Care and Use of Laboratory

Animals and approved by the Animal Ethics Committee of the Federal University of São Carlos (010/2011).

Anesthesia was induced by intra-peritoneal injection of Ketamine (Agener®, 40 mg/kg, IP) and Xylazine (Syntec®, 20 mg / kg, IP). Bilateral bone defects (3.0 mm diameter) were surgically created at the tibia (10 mm distal of the knee joint). For this, the tibia was exposed through a longitudinal incision on the shaved skin. After expose the tibia, bone defect was created by using a motorized round drill (BELTEC®, Araraquara-SP, Brazil), under constant physiologic saline irrigation. After the defect creation, they were packed with sterile cotton gauze to stop bleeding. Thereafter, the cutaneous flap was replaced and sutured with resorbable Vicryl® 5-0 (Johnson & Johnson, St. Stevens-Woluwe, Belgium). The animals were divided into 2 groups (n=30 each group): bone defect control group (CG) (bone defects without any treatment) and bone defect laser irradiated group (LG). To minimize post-operative discomfort the animals received analgesia (i.m., 0,02 mg/kg buprenorfiine - Temgesic; Reckitt Benckiest Healt Care Ltd. Schering-Plough, Hoddesdon,Uk) directly after the operation and subcutaneously for 2 days after surgery. Rats were euthanized individually by carbon dioxide asphyxia in different set points (36 hours, 3 days and 7 days after surgery).

4. 3.2 Low Level Laser Therapy

A laser (Thera laser, DMC® São Carlos, Brazil), CW, 830 nm, 0.6 mm beam diameter, 30 mW, 94 s, 2.8 J, 100 J/cm² was used in this study. LLLT sessions started immediately after the surgery and it was repeated each 24 hours for two, three or seven

days. Treatments were performed by the contact technique, at one point, above of the site of the injury.

4.3.3 Retrieval of specimens

The right tibias, used for gene expression evaluation (n=10 per group), were dissected, rapidly frozen in liquid nitrogen and stored in freezer at -80 °C until *microarray* analysis. For histopathological analysis, the left tibias (n=10 per group), after removal, were immediately fixed in 10% formaldehyde (Merck, Darmstadt, Germany) for 24 hours, followed by decalcified in 4% diamine tetra-acetic acid (EDTA) (Merck, Darmstadt, Germany) and embedded in paraffin blocks. Therefore, thin sections (5 μm) were prepared in the longitudinal plane, using a micrometer (Leica RM—2145, Germany). After, laminas were stained with hematoxylin and eosin (H.E stain, Merck, Darmstadt, Germany).

4. 3.4 Histopathological analysis

A descriptive qualitative histopathological evaluation of the total area of the bone defect was performed by two experienced observers (PB and CT) in a blinded manner, under a light microscope (Olympus, Optical Co. Ltd, Tokyo, Japan).[19,21] Any changes in the bone defect, such as presence of blood clot, fibrin, inflammatory process, granulation tissue, woven bone, or even tissues undergoing hyperplastic, metaplastic and/or dysplastic transformation were investigated per animal.

4. 3.5 RNA sample preparation

Total RNA was isolated using the TRIzol® reagent (Invitrogen, Carlsbad, California) according to the manufacturer's instructions. After the RNA isolation, the samples was purify using the illustra RNAspin Mini RNA Kit (GE Healthcare Life Sciences, USA) according to the manufacturer's instructions. The RNA concentrations were determined using a NanoVue spectrophotometer (GE Healthcare Life Sciences, USA). The quality and integrity of the total RNA were evaluated with an Agilent 2100 Bioanalyzer (GE Healthcare Life Sciences, USA) and sample presenting RNA integrity number ≥ 8 were used for cRNA synthesis.

4.3.6 *Microarray* hybridizations

Microarray hybridizations were performed with Agilent Whole Rat Genome *Microarray* 4x44 K. The labeling and *microarray* hybridizations were performed by Agilent using Two-Color *Microarray*-Based Gene Expression Analysis (Agilent Technologies, USA). Briefly, for cDNA synthesis and labeling 200 ng of total RNA were used. After, cDNA was transcribed into cRNA and it was labeled using Agilent Low RNA input Fluorescent Linear Amplification Kit (Agilent Technologies, Santa Clara, CA, USA). Then, cRNA labeled were purified, mixed with hybridization buffer and hybridized to an Agilent Whole Rat Genome *Microarray* 4x44 K for 17 hours at 65°C, according to the manufacturer's instructions. After hybridization, *microarray*s were sequentially washed: 1 minute at room temperature with GE Wash Buffer 1 (Agilent Technologies, USA) and 1 minute with 37°C GE Wash buffer 2 (Agilent Technologies, USA), then a 10 seconds Acetonitrile Wash (Agilent Technologies,

USA), followed by a 30 seconds Stabilization and Drying Solution wash (Agilent Technologies, USA). Afterwards, *microarray* slides were scanned using GenePix® 4000B *microarray* scanner (Molecular Devices, USA) with simultaneously scanning the Cy3 and Cy5 channels at a resolution of 5 μm. Laser was set at 100% and PMT gain was adjusted automatically for each slide using the program GenePix 4000B according to the signal intensity of each array.

4.3.7 *Microarray* data analysis

Microarray data analysis was performed as described by Castro *et al*.,[27]. Data files were generated using Agilent′s Feature Extraction Software (version 11.5, Agilent) and the default parameters, which include Lowess based signal normalization. The dye-normalyzed values generated in the Feature Extraction data files were used to upload the software Express Converter (version 2.1, TM4 available at http://www.tm4.org/utilities.html) which conveniently converts the Agilent file format to MeV (MultiExperiment View) file format compatible to the TM4 softwares for *microarray* analysis (available at http://www.tm4.org/). The MeV files were then uploaded in the MIDAS software where the resulting data were averaged from replicated genes on each array, from tree biological replicates, taking a total of 3 intensity data points for each gene. The MeV files generated were then loaded in MeV software where differentially expressed genes were identified using one-class t-test ($p>0.01$). Significantly different genes were those whose mean log2 expression ratio over all included samples was statistically different from 0 which indicates the absence of gene modulation.

4.3.8 Functional Analyses Using Ingenuity Pathways Analysis (IPA) Software

A network analysis was performed using the Ingenuity Pathways Analysis (IPA) (Ingenuity Systems, www.ingenuity.com) algorithm. The lists of differentially expressed genes were entered into the IPA software to explore relevant biological networks and to assess interactions with other genes. A hypothetical global gene interaction network was constructed, showing the most relevant direct and indirect connections of genes found to be regulated under LLLT.

4.3.9 Quantitative real-time polymerase chain reaction (RT-PCR)

RT-PCR was performed to confirm the differential expression results obtained by the *microarray* experiments. Total RNA was extracted and purified using the experimental protocols described above. One microgram of total RNA was reverse-transcribed into cDNA, and followed by RT- PCR amplification using rats gene-specific *primer*s (Table 2), which were designed by *Primer*Express Software (Applied Biosystems, Foster City, CA, USA). The optimized PCR conditions were: initial denaturation at 94 °C for 10 min, followed by 40 cycles consisting of denaturation at 94 °C for 15 s, annealing at 60 °C for 1 min, and extension at 72 °C for 45 s, with a final extension step at 72 °C for 2 min. Negative control reactions with no template (deionized water) were also included in each run. For each gene, all samples were amplified simultaneously in duplicate in one assay run. Analysis of relative gene expression was performed using the 2-ΔΔCT method. RPS18 was used as a housekeeping gene to normalize our expression data.

Table 2. Real-time PCR *Primer*s

Gene	Forward *primer*	Reverse *primer*
RPS18	GTGATCCCCGAGAAGTTTCA	AATGGCAGTGATAGCGAAGG
PTGER2	GAACTGCGAGAGTCGTCAGTATCTC	CCCCGGCCGTGAACAT
IL1R1	AAGTGGAATGGGTCGGAAATT	TGAAGGGTGTTCCAAAAACTGA
ANGPT4	GGCATCTACTATCCGGTTCATCA	CATGCGTGTGCCATGCA
PDGFD	TATGCTCATTGGATGCCTTGTC	TGCTGCTATCGGGACACTTTT
FGF2	AAGGATCCCAAGCGGCTCTA	CGGCCGTCTGGATGGA

4.3.10 Immunohistochemistry

After deparaffinization and rehydration in graded ethanol, each specimen was pretreated in a Steamer with buffer Diva Decloaker (Biocare Medical, CA, USA) for 5 min for antigen retrieval. The material was pre-incubated with 0.3% hydrogen peroxide in phosphate-buffered saline (PBS) solution for 30 min in order to inactivate endogenous peroxidase and then block with 5% normal goat serum in PBS solution for 20 min. Three sections of each specimen were incubated with anti-Cyclooxygenase-2 (COX-2, Cat. n° sc-1747) polyclonal primary antibody and anti-Vascular endothelial growth factor (VEGF, Cat. n° sc-1881) polyclonal primary antibody, both at a concentration of 1:200 (Santa Cruz Biotechnology, Santa Cruz, USA). Incubation was performed overnight at 4°C in refrigerated environment. Afterwards, two washes were done in PBS for 10 min. Then, incubation of the sections was performed making use of biotin conjugated secondary antibody anti-rabbit IgG (Vector Laboratories, Burlingame, CA, USA) at a concentration of 1:200 in PBS for 30 min. The sections were washed twice with PBS followed by the application of preformed avidin biotin complex conjugated to peroxidase (Vector Laboratories, Burlingame, CA, USA) for 30 min. The bound complexes were visible by the application of a 0.05% solution of 3-3′-

diaminobenzidine solution and counterstained with Harris hematoxylin. In order to carry out control studies of the antibodies, the serial sections were treated with rabbit IgG (Vector Laboratories, Burlingame, CA, USA) at a concentration of 1:200 instead of the primary antibody. Furthermore, internal positive controls were performed with each staining bath.

COX-2 and VEGF immunoexpression was assessed both qualitatively (presence of the immunomarkers) and semi-quantitatively in five pre-determined fields using a light microscopy (Leica Microsystems AG, Wetzlar, Germany) according to a previously described scoring scale ranging from 1 to 4 (1=absent, 2= slight, 3=moderate and 4=intense) for immunohistochemical analysis.[21] The analysis was performed by 2 observers (PB and CT), in a blinded way.

4.4 Statistical analysis

The normality of all variables distribution was verified using Shapiro–Wilk's W test. For immunohistochemical analysis, comparisons among groups were performed using one-way analysis of variance (ANOVA), complemented by Tukey post-test analysis. STATISTICA version 7.0 (data analysis software system - StatSoft Inc.) was used to carry out the statistics analysis. Values of $p<0.05$ were considered statistically significant.

4.5 RESULTS

4.5.1 Histopathological analysis

Representative histological images of all experimental groups are depicted in Figure 4.

Thirty-six hours after surgery, histology assessment for CG revealed that bone defect area was filled with blood clotting and inflammatory tissue, including polymorphonuclear cells (Figure 4A). At the same period, for LG, an intense inflammatory process filled bone defect area. Furthermore, some granulation tissue, mainly at the periphery of the defect, was observed (Figure 4B). Figure 4C shows that, 3 days after surgery, in the CG, inflammatory cells still could be observed, especially in the central region of the defect. Moreover, most of the injury area was filled by granulation tissue and immature newly formed bone surrounding the border (Figure 4C). For LG, some inflammatory cells were still observed. Most all of the defect was filled by granulation tissue and immature newly formed bone at the periphery (Figure 4D).

On day 7 after surgery, in CG, granulation tissue was present in almost all defect area. Some immature newly formed bone was seen in the peripheral area of the injury (Figure 4E). At the same period, histology assessment revealed an absence of inflammatory processes in LG. In addition, the bone defects were filled with newly formed bone, with interconnected concentric trabeculaes. Areas of granulation tissue still could be observed. (Figure 4F).

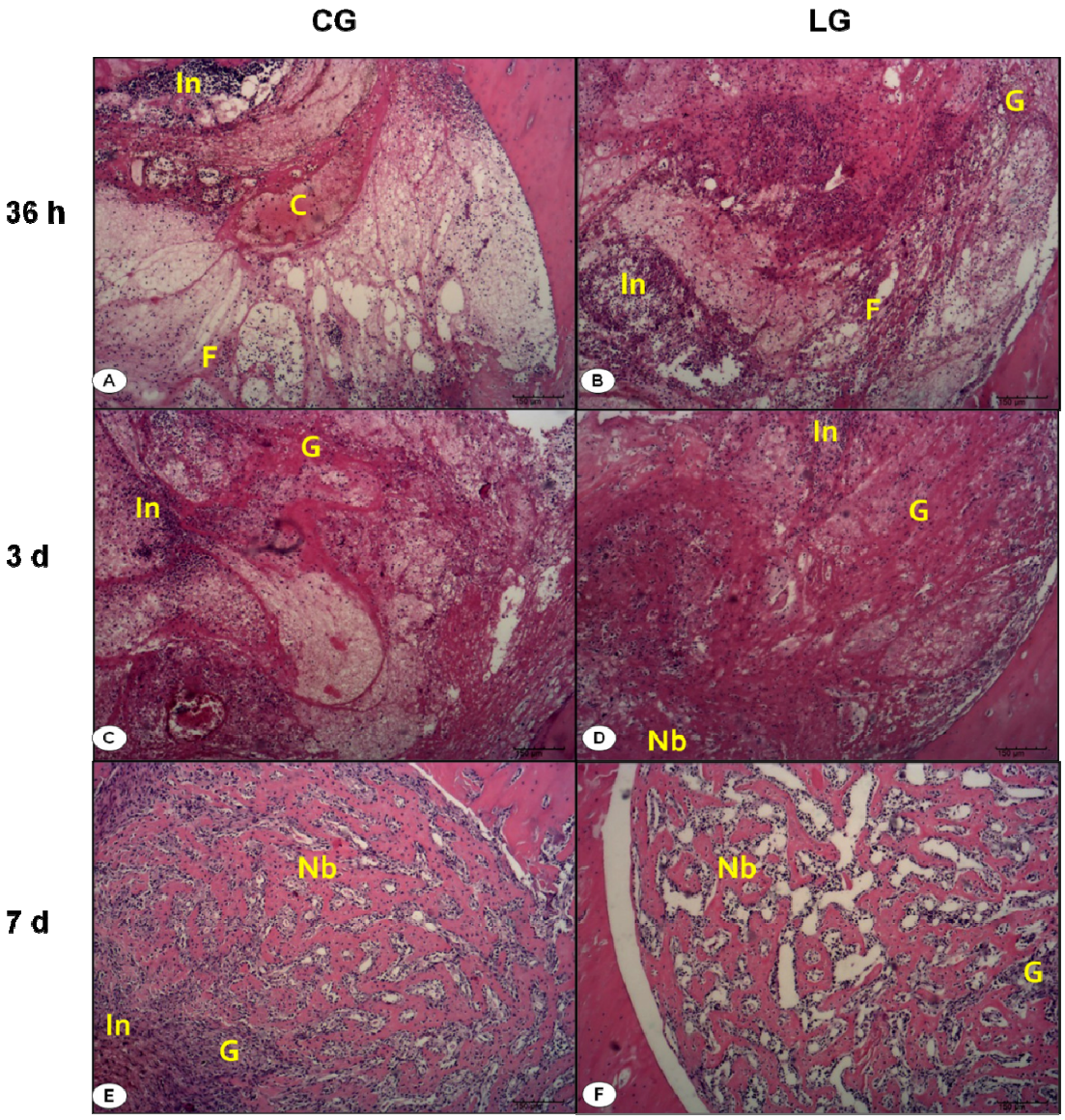

Figure 4. Representative histological sections of experimental groups showing newly formed bone (Nb), fibrin (F), granulation tissue (G), inflammatory infiltrate (In), blood clot (C). (Hematoxylin and Eosin stain; scale bar = 150 µm).

4.5.2. *Microarray* Analysis

After sorting through the *microarray* analysis, a total of 5.765 genes modulated by LLLT, in the 3 experimental periods, were identified and organized in a hierarchical cluster.

4.5.2.1. Functional network analysis

In order to further refine the significance of the regulated genes in LG, possible biological interactions using the IPA software tool were investigated. Several networks that may be involved in bone healing were identified. In particular, networks associated to inflammatory response, connective tissue development and skeletal and muscular system activity were investigated (table 3).

Table 3. Top Genetic network

	Network Functions	Score
36 hours		
	Cellular Movement, Hematological System Development and Function, Immune Cell Trafficking.	28
	Cellular Movement, Hematological System Development and Function, Hypersensitivity Response.	24
	Cellular Assembly and Organization, Cellular Function and Maintenance, Cellular Movement.	22
Day 3		
	Inflammatory Response, Cellular Development, Hematological System Development and Function.	31
	Cellular Compromise, DNA Replication, Recombination, and Repair, Molecular Transport.	19
	Cellular Development, Cell Cycle, Connective Tissue Development and Function.	17
Day 7		
	Cellular Development, Hematological System Development and Function, Hematopoiesis.	26
	Cell Morphology, Tissue Development, Cellular Movement.	24
	Cell Morphology, Cellular Assembly and Organization, Organismal Injury and Abnormalities.	22

After merging the networks listed in Table 3, several canonical pathways were obtained, which were based on their functional annotations and known molecular interactions by IPA. Thus, several functional groupings of differentially expressed

genes were identified. However this report focused on early events of bone healing, including inflammation and angiogenesis, which is most active in the recruitment of cells and release of various cytokines/growth factors, and thus represents a stage of fracture healing.

The up-regulated and down-regulated inflammatory and angiogenesis genes were further examined and revealed some COX-2 related genes, interleukins, growth factors, angiopoietin and VEGF signaling and provided an initial analysis.

The inflammatory and angiogenic genes were significantly up-regulated at 36 hours and 3 days after surgery, followed by a down regulation of the genes on day 7, which suggests that inflammatory and angiogenic responses may have been modulated by LLLT (table 4).

Table 4. List of chosen genes modulated after LLLT irradiation

Function	Gene Symbol	Description	Fold Change
		36 hours	
Inflammation	PTGIR	prostaglandin I2 (prostacyclin) receptor	1.043
	PTGS-2	prostaglandin-endoperoxide synthase 2 (prostaglandin G/H synthase and cyclooxygenase)	1.159
	MMD	monocyte to macrophage differentiation-associated	2.07
	IL-18	interleukin 18	2.483
	IL-1	interleukin 1	1.703
Angiogenesis	FGF-14	fibroblast growth factor 14	2.361
	FGF-2	fibroblast growth factor 2	3.163
	FGFBP-1	fibroblast growth factor binding protein 1	2.128
	ANGPT-2	angiopoietin 2	2.84
		Day 3	
Inflammation	PTGER-2	prostaglandin E receptor 2	3.226
	PTGIR	prostaglandin I2 (prostacyclin) receptor	-2.322
	IL-4	interleukin 4	2.899
Angiogenesis	ANGPT-4	angiopoietin 4	1.098
	PDGFD	platelet derived growth factor D	1.319
	FGFR-2	fibroblast growth factor receptor 2	-1.023
		Day 7	
Inflammation	PTGFR	prostaglandin F receptor (FP)	-1.079
	PTGIR	prostaglandin I2 (prostacyclin) receptor (IP)	-1.815
	PTGS-1	prostaglandin-endoperoxide synthase 1 (prostaglandin G/H synthase and cyclooxygenase)	-2.738
	IL-18	interleukin 18 (interferon-gamma-inducing factor)	-2.779
	IL-1	interleukin 1	-2.564
Angiogenesis	ANGPT-2	angiopoietin 2	-3.692
	PDGFD	platelet derived growth factor D	-2.025
	PDGFRA	platelet-derived growth factor receptor, alpha polypeptide	-3.751

4.5.2.2. Validation of *microarray* data by real-time PCR

In order to validate the results of the *microarray* assays, the SYBR Green-based real-time PCR on control and irradiated group was performed. The genes were selected according to the canonical pathway analysis and the references in previous studies

(Kido *et al*., 2014; Favaro-Pipi *et al* 2011). The expression profiles of the genes confirmed the *microarray* results.

4. 5.3. Immunohistochemistry analysis

4. 5.3.1. COX-2 expression

Qualitative immunohistochemical analysis demonstrated that in the first and second experimental periods, COX-2 expression was predominantly detected in granulation tissue for both groups (Figures 5A). Seven days post-surgery, for CG, the immunoreactivity of COX-2 was mainly observed in granulation tissue. For the LG, COX-2 immunolabeling was observed in granulation and in the osteoblastic cells.

Semi-quantitative analysis revealed a significant increase in COX-2 immunoexpression was observed in the LG compared to CG, 36 hours after surgery. On day 3, no statistical difference was observed between CG and LG. Moreover, COX-2 immunoexpression was higher in CG compared to LG on day 7 (Figure 5B).

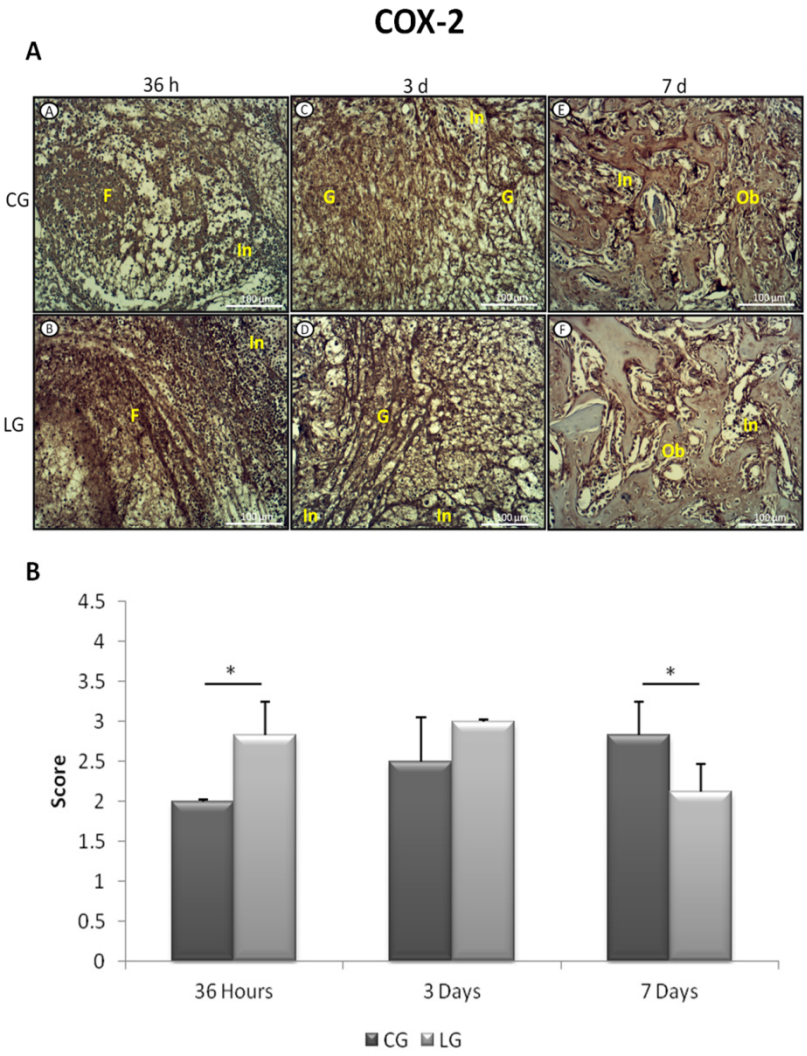

Figure 5. **A** Representative sections of COX-2 immunohistochemistry. Fibrin (F), granulation tissue (G), inflammatory infiltrate (In), osteoblastic cells (Ob). **B** Means and standard error of the mean of scores immunohistochemistry of COX-2. Significant differences of $p < 0.05$ are represented by a single asterisk (*).

4.5.3.2 VEGF expression

Qualitative immunohistochemical analysis demonstrated that VEGF expression was predominantly observed in the capillary walls and granulation tissue for both experimental groups 36 hours after the surgery. On days 3 and 7 after surgery, the

immunoexpression of VEGF was identified in the capillary walls, granulation tissue and osteoblastic cells for both groups (Figures 6A).

Semi-quantitative analysis demonstrated that VEGF immunoexpression was similar between CG and LG, 36 hours after the surgery. On days 3 and 7, LG presented a significantly higher up-regulation of VEGF compared to the CG (Figure 6B).

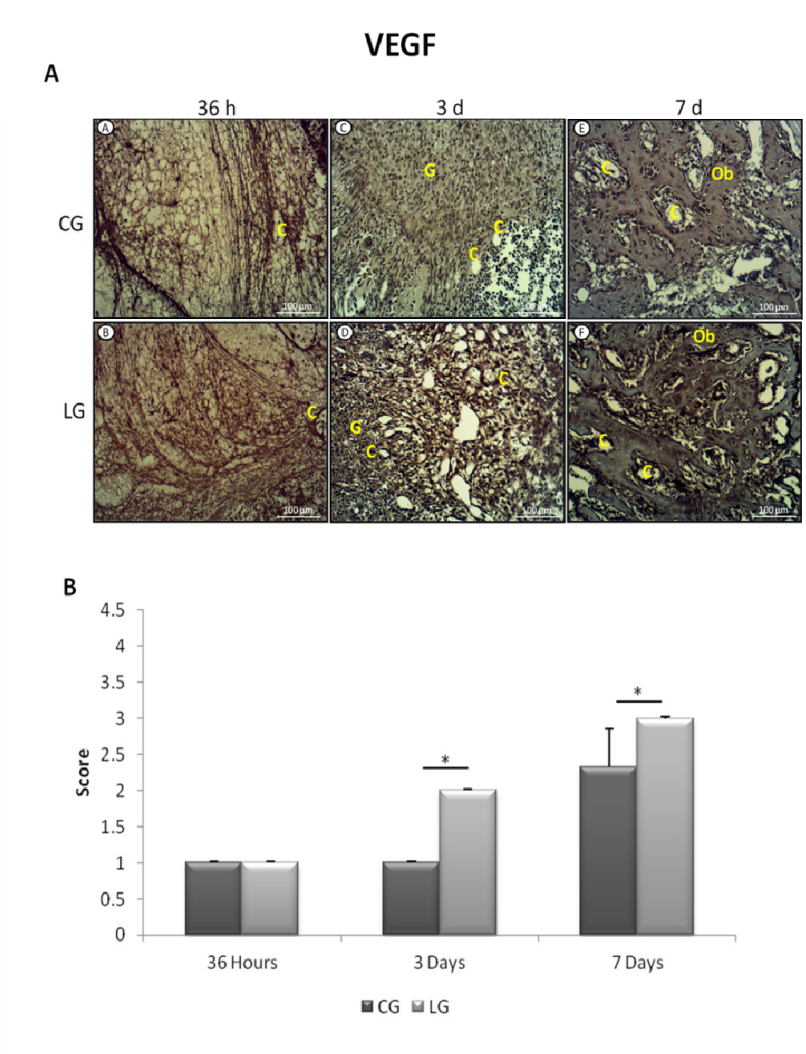

Figure 6. A Representative sections of VEGF immunohistochemistry. Capillary (C), granulation tissue (G), osteoblastic cells (Ob). **B** Means and standard error of the mean of scores immunohistochemistry of VEGF. Significant differences of $p < 0.05$ are represented by a single asterisk (*).

4.6. DISCUSSION

This study aimed to investigate the effects of LLLT on the morphological aspects of bone callus and on gene and immunomarker expression related to the inflammatory process and angiogenesis during the initial phase of bone healing in a model of tibial bone defect in rats. The main findings showed that LLLT produced an earlier recruitment of inflammatory cells, as well as increased amount of newly formed bone at the site of the injury. Furthermore, our results evidenced that LLLT produced a significantly increase in the expression of genes related to inflammation and angiogenesis. The immunoexpression of COX-2 (36 hours) and VEGF (3 and 7 days) were also increased in the laser treated animals.

Increased cell proliferation and acceleration of tissue metabolism are the most important physiological effects of LLLT, contributing to the stimulation of healing after an injury.[31] In this context, several studies demonstrated that LLLT had a positive effect in the process of bone consolidation in experimental models in rats.[19,21,28] Fernandes *et al.*[29] showed that LLLT induced a recruitment of inflammatory cells and increased newly formed bone in the initial phases of bone consolidation. These findings are in line with the results of the current study, which the histological analysis revealed that LLLT improved the biological response of bone tissue by modulating the inflammatory process and stimulating the deposition of newly formed bone at the site of the injury. It seems that LLLT can stimulate osteogenic genes that are involved in bone repair, which may explain the positive results of this therapy on bone healing, with the modulation of the inflammatory process and the earlier recruitment of osteoprogenitor cells, thus increasing the rate of bone formation and bone ingrowth into the defect area.[30]

In addition, *microarray* analysis suggest that LLLT could have stimulated the healing process and accelerated the process of bone healing by a down-regulation of pro-inflammatory interleukins (IL1, 1IL6, IL8, IL18) at 36 hours after the surgery, followed by up-regulation of anti-inflammatory interleukin (IL4) on day 3. Furthermore, inflammatory cells such as macrophages, neutrophils and fibroblasts are activated to remove damaged tissue and stabilize the blood clot.[32] In the present study, it was observed increased activity of monocyte to macrophage differentiation-associated gene (MMD), which could be directly related to the up-regulation of prostaglandins genes (PTGIR, PTGS2, Ptger2) observed in LG at 36 hours and day 3 after surgery, that may also have contributed to the acceleration of bone repair observed in the irradiated animals. Specifically in bone healing, prostaglandins (PGs) and arachidonic acid products play a key role in the generation of the inflammatory response and the enzyme responsible for this process (convert arachidonic acid to prostanoids) is the cyclo-oxygenase.[33] Additionally, effects of LLLT on the modulation of inflammation were also demonstrated by the increased immunoexpression of COX-2 in the LG in the first experimental period followed by a decreased immunoexpression. This results suggest that LLLT modulates the synthesis of inflammatory mediators which can culminate in the earlier resolution of the inflammatory process observed in the LG, and consequently, may have anticipated the steps of tissue repair, as was demonstrated in histopathological analysis. Some authors have postulated that the early modulation of pro-inflammatory mediators can prevent excess tissue degradation. This modulation can also stimulate the bone repair.[19] There are several reports highlighting LLLT effects in inflammatory modulation.[34-36] Recently, Rambo *et al*.,[37] observed that LLLT was effective in decreasing the expression on the pro-inflammatory mediators (IL-1 and TNF) and it was able to increase expression of the anti-inflammatory cytokine IL-10.

Similarly, angiogenesis is an essential part of fracture repair.[4] Angiogenesis is not only responsible for the oxygen supply, but also a prerequisite for the resorption of necrotic tissue and recruitment of different cell types including mesenchymal progenitor cells, which is necessary for a mechanically stable repair of the bone defect.[5] In essence, FGF and PDGF are a required element in cellular division for fibroblasts, a type of connective tissue cell that is especially prevalent in wound healing. Also, it has important function in the promotion of endothelial cell proliferation.[38] In the present study, it was demonstrated that LLLT can stimulate angiogenic genes in injured tissues such as ANGPT2 and ANGPT4, at 36 hours and 3 days after surgery, respectively. In addition, our *microarray* findings showed that LLLT produced an up-regulation of FGF and PDGF at 36 hours and 3 days after surgery. Similarly, VEGF imunoexpression was increased after laser stimulation. These results are in agreement with those found by Bossini *et al*.,[19] who investigated the effects of LLLT in osteoporotic rats and concluded that LLLT improves bone repair as a result of stimulation of angiogenesis and newly formed bone.

Taken together, the results of the present study showed that LLLT might be promising to improve bone consolidation in the initial period of repair by modulating the expression of genes related to inflammation and neoangiogenesis, which may culminate in the stimulation of bone cells and increased newly formed bone. As this study was limited to a short-term evaluation, information about the influence of LLLT on gene expression in long-term analysis needs to be provided. Also, other molecular pathways such as the expression of genes related to the osteoblast differentiation remain to be investigated.

4.7 CONCLUSION

Summarizing, this study suggests that LLLT was efficient in modulating the inflammatory process and increasing the newly formed bone. In addition, LLLT produced a significant increase in the expression of genes related to inflammation and angiogenesis. This fact may explain some of the molecular pathways by which LLLT acts on the stimulation of bone tissue during the process of healing and result in the earlier resolution of the inflammatory process and earlier differentiation of pre-osteoblastic cells into mature osteoblasts, accelerating bone healing process. Consequently these data highlight the potential of LLLT to be used as a therapeutic approach for bone regeneration.

Acknowledgments

We would like to acknowledge the contributions of Brazilian funding agency Fapesp (2010/15335-0) and the Center for Computational Engineering and Sciences at UNICAMP SP Brazil (FAPESP/CEPID and project #2013/08293-7) for the financial support of this research.

4. 8 REFERENCES

1. C. Ferguson, E. Alpern, T. Miclau, and Helms J.A, "Does adult fracture repair recapitulate embryonic skeletal formation?," *Mech Dev*. **87**(1-2), 57-66 (1999).

2. R. Dimitriou, E. Tsiridis, and P. V. Giannoudis, "Current concepts of molecular aspects of bone healing," *Injury* **36**(12), 1392-404 (2005).

3. A. Tedgui, and Z. Mallat, "Anti-Inflammatory Mechanisms in the Vascular Wall" *Circ Res.* **11**(9), 877-87 (2001).

4. J. Street *et al*,."Is human fracture hematoma inherently angiogenic?," *Clin. Orthop.* **378** (9), 224–237 (2000).

5. R. A.D. Carano and E. H. Filvaroff, "Angiogenesis and bone repair," *Drug Discov Today* **8**(21), 980-9 (2003).

6. L.C. Gerstenfeld *et al*., "Fracture healing as a post-natal developmental process: molecular, spatial, and temporal aspects of its regulation," *J Cell Biochem.* **88**(5), 873–884 (2003).

7. M.E. McGee-Lawrence , and D.F. Razidlo, "Induction of fully stabilized cortical bone defects to study intramembranous bone regeneration,**"** *Methods Mol Biol*. 1226, 183-92 (2014).

8. G. Victoria *et al*., "Bone stimulation for fracture healing: what's all the fuss?," *Indian J. Orthop.* **43**(2), 117–120 (2009).

9. A.N. Silva Júnior *et al*., "Computerized morphometric assessment of the effect of low-level laser therapy on bone repair: an experimental animal study," *J Clin* Laser *Med Surg.* **20**(2), 83-7 (2002).

10. L.A. Merli *et al*., "Effect of low-Intensity laser irradiation on the process of bone repair," *Photomed* Laser *Surg.* **23**(2), 212-5 (2005).

11. O. Dortbudak, "Biostimulation of bone marrow cells with a diode soft laser," *Clin. Oral Implants Res.* **11**(16), 540–545 (2000).

12. T. Karu, "Primary and secondary mechanisms of action of visible to near-IR radiation on cells," *J Photochem Photobiol. B* **49**(1), 1-17 (1999).

13. D. Hawkins and H. Abrahamse, "Effect of multiple exposures of low level laser therapy on the cellular responses of wounded human skin fibroblasts," *Photomed* Laser *Surg.* **24**(6), 705-714 (2006).

14 W.P. Hu *et al*., "Helium- Neon Laser Irradiation Stimulates Cell Proliferation through Photostimulatory Effects in Mitochondria," *J Investigat Dermatol.* **127**(8), 2048-57 (2007).

15. E.M. Laraia *et al*., "Effect of low-level laser therapy (660 nm) on acute inflammation induced by tenotomy of Achilles tendon in rats," *Photochem Photobiol.* **88**(6), 1546–50 (2012).

16. F.M. de Lima *et al*., "Dual Effect of low-level laser therapy (LLLT) on the acute lung inflammation induced by intestinal ischemia and reperfusion: action on anti- and pro-inflammatory cytokines," Laser*s Surg Med*. **43**(5), 410–20 (2011).

17. F. Mafra de Lima *et al*., "Low intensity laser therapy (LLLT) *in vivo* acts on the neutrophils recruitment and chemokines/cytokines levels in a model of acute pulmonary

inflammation induced by aerosol of lipopolysaccharide from Escherichia coli in rat," *J Photochem Photobiol. B* **101**(3), 271–8 (2010).

18. A.S. da Rosa *et al*., "Effects of low-level laser therapy at wavelengths of 660 and 808 nm in experimental model of osteoarthritis," *Photochem Photobiol.* **88**(1), 161–6 (2012).

19. P.S. Bossini *et al*., "Low level laser therapy (830nm) improves bone repair in osteoporotic rats: similar outcomes at two different dosages," *Exp Gerontol.* **47**(2), 136-42 (2012).

20. A.V. Corazza *et al*., "Photobiomodulation on the angiogenesis of skin wounds in rats using different light sources" *Photomed.* Laser *Surg.* **25**(2), 102-6. (2007).

21. C.R. Tim *et al*., "Low-level laser therapy enhances the expression of steogenic factors during bone repair in rats," Laser*s Med Sci.* **29**(1), 147-56 (2013).

22. L. Assis *et al*., "Low-level laser therapy (808 nm) reduces inflammatory response and oxidative stress in rat tibialis anterior muscle after cryolesion," Laser*s Surg Med.* **44**(9), 726-35 (2012).

23. A. Stein *et al*., "Low level laser irradiation promotes proliferation and differentiation of human osteoblasts *in vitro*," *Photomed* Laser *Surg.* **23**(2), 161-6 (2005).

24. K. Sena *et al*., "Early gene response to low-intensity pulsed ultrasound in rat osteoblastic cells," *Ultrasound Med. Biol.* **31**(5), 703–708 (2005).

25. Y. A. Vladimirov, A. N. Osipov, and G. I. Klebanov, "Photobiological principles of therapeutic applications of laser radiation," *Biochemistry* **69**(1), 81–90 (2004).

26. J. Zhao *et al*., "Transcriptome analysis of β-TCP implanted in dog mandible," *Bone* **48**(4), 864-77 (2011).

27. P.A. de Castro *et al*., "Transcriptional profiling of Saccharomyces cerevisiae exposed to propolis," *BMC Complement Altern Med.* **24**(12), 194 (2012).

28. M.A. Matsumoto *et al*., "Low-level laser therapy modulates cyclo-oxygenase-2 expression during bone repair in rats," Laser*s Med Sci.* **24**(2), 195-201 (2009).

29. K.R. Fernandes , *et al*., "Effects of low-level laser therapy on the expression of osteogenic genes related in the initial stages of bone defects in rats," *J Biomed Opt*. **18**(3), 038002 (2013).

30. E. Fávaro-Pípi *et al*., " Low-level laser therapy induces differential expression of osteogenic genes during bone repair in rats," *Photomed* Laser *Surg.* **29**(5), 311-7 (2011).

31. Y.H. Wu *et al*., "Effects of low-level laser irradiation on mesenchymal stem cell proliferation: a *microarray* analysis," Laser*s Med Sci.* **27**(2), 509-19 (2012).

32. L.J. Raggatt ,*et al*., "Fracture Healing via Periosteal Callus Formation Requires Macrophages for Both Initiation and Progression of Early Endochondral Ossification," *Am J Pathol.* **9440**(14), 00504-5 (2014).

33. X. Zhang et ., "Cyclo-oxygenase-2 regulates mesenchymal cell differentiation into the osteoblast lineage and is critically involved in bone repair," *J Clin Invest.* **109**(11), 1405-15 (2002).

34. T.Y. Fukuda *et al*., "Infrared low-level diode laser on inflammatory process modulation in mice: pro- and anti-inflammatory cytokines," Laser*s Med Sci.* **28**(5), 1305-13 (2013).

35. V.S. Hentschke *et al*., "Low-level laser therapy improves the inflammatory profile of rats with heart failure," Laser*s Med Sci.* **28**(3), 1007-16 (2012).

36. K. P. S. Fernandes *et al*., "Effect of photobiomodulation on expression of IL-1β in skeletal muscle following acute injury**,"** Laser*s Med Sci.* **28**(3), 1043-6 (2013).

37. C. S. M. Rambo *et al*., "Comparative analysis of low-level laser therapy (660 nm) on inflammatory biomarker expression during the skin wound-repair process in young and aged rats," Laser*s Med Sci.* **29**(5), 1723-33 (2014).

38. J.R. Lieberman, A. Daluiski, and T.A. Einhorn, "The role of growth factors in the repair of bone. Biology and clinical applications," *J Bone Joint Surg.* **84**-A(6), 1032-44 (2002).

5. ESTUDO 2

Effects of low level laser therapy on the expression of osteogenic genes during the initial stages of bone healing in rats: a *microarray* analysis

Carla Roberta Tim[1], Paulo Sérgio Bossini[2], Hueliton Wilian Kido[1], Iran Malavazi[3], Marcia Regina von Zeska Kress[4], Marcelo Falsarella Carazzolle[5,6], Nivaldo Antonio Parizotto[1], Ana Cláudia Rennó[2].

[1]Federal University of São Carlos, Department of Physiotherapy, Rod Washington Luis Km 235, São Carlos, Brazil, 13565-905.
[2]Federal University of São Paulo, Department of Bioscience, Av. Ana Costa 95, Santos, Brazil, 11050-240.
[3] Federal University of São Carlos, Department of Genetics and Evolution, Rod Washington Luis Km 235, São Carlos, Brazil, 13565-905.
[4] University of São Paulo, School of Pharmaceutical Sciences of Ribeirão Preto, Department of Clinical Analysis, Toxicological and Bromatological, Av. do Café 95, Ribeirão Preto, Brazil, 14049-900, Brazil
[5]State University of Campinas, Department of Genetics and Evolution, Cidade Universitária Zeferino Vaz, Campinas, Brazil, 13083-970.
[6]Brazilian National Center for Research in Energy and Materials, Brazilian Biosciences National Laboratory, Giuseppe Máximo Scolfaro 10.000, Campinas, Brazil, 13083-970.

5.1 Abstract: This study evaluates the morphological changes produced by LLLT on the initial stages of bone healing and to studies the pathways that stimulate the expression of genes related to bone cell proliferation and differentiation. One hundred Wistar rats were divided into control and treated groups. Noncritical size bone defects were surgically created at the upper third of the tibia. Laser irradiation (Ga-Al-As laser 830 nm, 30 mW, 94 s, 2,8 J, 100 J/cm² was performed for 1, 2, 3, 5 and 7 sessions. Histopathology revealed that treated animals produced increased amount of newly formed bone at the site of the injury. Also, *microarray* analysis evidenced that LLLT produced a significantly increase in the expression TGF, BMP, FGF and RUNX-2 that could stimulate osteoblast proliferation and differentiation, which may be related to improving the deposition of newly formed bone at the site of the injury. Thus, it is possible to concluded that LLLT improves bone healing by producing a significant increase in the expression of osteogenic genes.

Key words: bone regeneration, LLLT, *microarray*, osteogenic genes.

5.2. INTRODUCTION

It is estimated that approximately six million fractures happen annually only in the United States [1]. In general, bone tissue has the ability of healing by itself [2]. However, between 5–10 % of fractures result in delayed union or nonunion depending on the extension of the injury or its association to diseases and therefore result in high health care costs [3]. In this context, the clinical demand for therapeutic strategies to promote bone repair has been growing in recent years in direct relation to the increase on the human population [4]. One of the most promising treatments is the use of low level laser therapy (LLLT), which is able of reestablishing cellular homeostasis and regenerating biological tissues, such as muscle, tendons, cartilage and bone [1,5-9].

The action of LLLT is based on the absorption of laser light by tissues, stimulating mitochondrial respiratory chain and, consequently ATP production [10]. These effects can increase the synthesis of DNA, RNA and cell-cycle regulatory proteins, therefore promoting cell proliferation [11, 12].

In bone tissue, *in vitro* and *in vivo* studies demonstrated that LLLT is able to up-regulate the expression of a series of growth factors, protein and genes related to bone cell differentiation, culminating in the stimulation of osteoblast proliferation and activity [13, 14]. Furthermore, LLLT modulates the expression of some inflammatory mediators such as Cyclooxygenase-2 (COX-2), tumor necrosis factor α (TNFα), interleukin 1β, (IL1β), and interleukin 10 (IL10) [7, 15, 16]. Moreover, it has been demonstrated that LLLT can stimulate VEGF expression and angiogenesis [6, 17]. Thus, this therapeutic modality has been used to promote wound healing, to accelerate tissue repair and to modulate the inflammatory process after injuries [7, 18].

A recent study demonstrated that LLLT increased the osteoblastic proliferation and gene expression of osteoblastic markers, such as alkaline phosphatase (ALP), runt-related transcription factor 2 (Runx-2), osteocalcin (OC), type I collagen (COL I), and bone sialoprotein (BSP) in osteoblasts cells derived from the midpalatal suture [19]. In addition, Wu *et al*., [14] used the *microarray* analysis to evaluate the gene expression of laser irradiated mesenquimal stem cells (MSCs) and demonstrated that various genes involved in cell proliferation, apoptosis and the cell cycle were up-regulated.

Despite the positive effects of LLLT on the stimulation of bone tissue, the molecular and cellular changes induced by this therapeutic approach on bone healing are not fully understood. Furthermore, the literature lacks descriptions on the mechanisms by which laser acts in the initial periods in LLLT repair, since most studies have evaluated its effects on intermediate and late periods of bone healing. Therefore, it is important to evaluate the early stages of bone repair such as blood clot formation, inflammatory processes and the deposition of newly formed bone tissues. These processes could stimulate the proliferation of different cells and signal molecules, which have the capacity to initiate the cascades of cellular events involved in bone repair and then stimulate the newly formed bone. In view of the aforementioned, it was hypothesized that LLLT could increase the expression of genes that stimulate osteoblast proliferation and differentiation, which may induce the bone formation and consequently accelerate the repair process.

In this context, the aim of the present study was to evaluate the morphological changes produced by LLLT on the initial stages of bone healing and to study the pathways that stimulate the expression of genes related to bone cell proliferation and differentiation. For this purpose, qualitative and quantitative histopathological analysis were used to evaluate the area of newly formed bone in an experimental tibial bone

defect model in rats. In order to study the global gene expression and thus provide significant insights about the genes regulated by LLLT during the initial process of bone healing *microarray* analysis was used.

5. 3 MATERIALS AND METHODS

5.3.1 Animals and study design

One hundred male Wistar rats, 12 weeks and weighing 250-300 g, were used in this study. The animals were distributed into 2 groups: bone defect control group (CG) (bone defects without any treatment) and bone defect laser irradiated group (LG). Each group was subdivided into five different sub-groups (N=20) and euthanized in different periods (12 hours, 36 hours, 3 days, 5 days and 7 days after surgery). All procedures were approved by institutional animal ethics committee of the Federal University of São Carlos (010/2011). All animal handling and surgical procedures were strictly conducted according to the Guiding Principles for the Use of Laboratory Animals.

5.3.2 Surgery to induce bone defects

At the beginning of the experiment, all animals underwent surgery to perform bone defects in tibias bilaterally. Surgery was performed under sterile conditions and general anesthesia induced by intra-peritoneal injection of Ketamine / Xylazine (80/10 mg/Kg). A 1 cm incision was made to expose the tibia and a standardized 3.0 mm diameter bone defect was created by using a motorized round drill under copious irrigation (12500 rpm) with saline solution. The incisions were sutured with resorbable

polyglactin, and the antisepsis was performed with poviddone iodine. The animals received analgesia (i.m., 0,05 mg/kg buprenorphine (Temgesic; Reckitt Benckiser Health Care Limited, Schering Plough, Hoddesdon, United Kingdom) and were returned to their cages. The health status of the rats was monitored daily [6,7].

5.3.3 Low Level Laser Therapy

Laser treated animals were submitted to LLLT using a low-energy Ga-Al-As, 830 nm (Thera laser, DMC® São Carlos - Brazil), continuous wavelength, 0.6 mm beam diameter, 30 mW, 94 s, 2,8 Joules, 100 J/cm². Laser irradiation started immediately after the surgery and it was performed for one (12 h), two (36 h), three (3 days), five (5 days) or seven (7 days) sessions, with an interval of 24 hours between each session. The application was punctual transcutaneously above the site of the injury.

5.3.4 Histopathological analysis

On the respective day, animals were euthanized individually by carbon dioxide asphyxia and both tibias were defleshed and removed for analysis. The left tibias were fixed in 10% formaldehyde (Merck, Darmstadt, Germany) for 24 hours, followed by decalcification in 4% diamine tetra-acetic acid (EDTA) (Merck, Darmstadt, Germany) and embedded in paraffin blocks. Sections (5 μm) were cut longitudinally and stained with hematoxylin and eosin (H.E stain, Merck, Darmstadt, Germany). Histopathological evaluation was performed under a light microscope (Olympus, Optical Co. Ltd, Tokyo, Japan.). Changes in the bone defect area, such as presence of blood clot, fibrin, inflammatory process, granulation tissue, woven bone, or even tissues undergoing

hyperplastic, metaplastic and/or dysplastic transformation were investigated in each animal [6,7].

5.3.5 Morphometry analysis

Using computer-based image analysis techniques (Motican 5.0, Meiji camera, Santa Clara - CA, USA), all histological sections were digitalized (10x magnification). The analysis was performed by 2 observers, in a blinded way (CT and PSB). From digitalized images of the defect, the amount of newly formed bone was determined within 5 regions of interest, i.e.: ROI1 (upper region of the border), ROI2 (right border), ROI3 (bottom region of the border), ROI4 (left border) and ROI5 (central region of the bone defect). This analysis was established in a previous study conducted by our team [9,11]. The amount of newly formed bone was determined in μm^2 in each ROI and the total newly formed bone was represented as ROI1+ROI2+ROI3+ ROI4+ ROI5.

5.3.6 Gene Expression Methods

5.3.6.1 RNA extraction, purification, yield and purity

RNA was extracted from right tibias and this process was performed using TRIzol reagent according to the manufacturer's instructions. Total RNA was purified by illustra RNAspin Mini RNA Kit (GE Healthcare Life Sciences, USA) according to the manufacturer's specifications, quantified by NanoVue spectrophotometer (GE Healthcare Life Sciences, USA) and its integrity confirmed by Agilent 2100

Bioanalyzer (GE Healthcare Life Sciences, USA) and sample presenting RNA integrity number ≥ 8 were used for cRNA synthesis.

5.3.6.2 *Microarray* hybridizations

The protocol for *microarray* processing was carried out according to Agilent using Two-Color *Microarray*-Based Gene Expression Analysis (Agilent Technologies, USA). Briefly, for cDNA synthesis and labeling 200 ng of total RNA were used. After, cDNA was transcribed into cRNA and it was labeled using Agilent Low RNA input Fluorescent Linear Amplification Kit (Agilent Technologies, Santa Clara, CA, USA). Then, cRNA labeled were purified, mixed with hybridization buffer and hybridized to an Agilent Whole Rat Genome *Microarray* 4x44 K for 17 hours at 65°C, according to the manufacturer's instructions. The hybridized *microarray*s were washed as the manufacturer's washing protocol (Agilent Technologies, Santa Clara, CA, USA).

5.3.6.3 Data acquisition and analysis

Afterwards, *microarray* slides were scanned using GenePix® 4000B *microarray* scanner (Molecular Devices, USA) with simultaneous scans of the Cy3 and Cy5 channels at a resolution of 5 μm. Laser was set at 100% and PMT gain was adjusted automatically for each slide using the program GenePix 4000B according to the signal intensity of each array.

Microarray data analysis was performed as described by Castro *et al*., [20]. Data files were generated using Agilent′s Feature Extraction Software (version 11.5, Agilent) and the default parameters, which include Lowess based signal normalization. The dye-

normalyzed values generated in the Feature Extraction data files were used to upload the software Express Converter (version 2.1, TM4 available at http://www.tm4.org/utilities.html) which conveniently converts the Agilent file format to mev (multi experiment view) file format compatible to the TM4 softwares for *microarray* analysis (available at http://www.tm4.org/). The MeV files were then uploaded in the MIDAS software where the resulting data were averaged from replicated genes on each array, from tree biological replicates, taking a total of 3 intensity data points for each gene. The MeV files generated were then loaded in MEV software (MultiExperiment Viewer) where differentially expressed genes were identified using one-class t-test ($p>0.01$). Thereafter, the genes statistically significant were those whose mean log2 expression ratio over all included samples was statistically different from 0 which indicates the absence of gene modulation.

5.3.6.4 Functional Analyses Using Ingenuity Pathways Analysis (IPA) Software.

Ingenuity Pathways Analysis version 4.0 (Ingenuity Systems, Mountain View, CA, USA) was used to search for possible biological processes, pathways and networks. By comparing the imported *microarray* data with the IKB, the list of genes was transformed into a set of relevant networks, focus genes and canonical pathways, and functionally annotated. A hypothetical global gene interaction network was constructed, showing the most relevant direct and indirect connections of genes found to be regulated under LLLT.

5.3.6.5 Quantitative real-time polymerase chain reaction (RT-PCR)

RT-PCR was performed to confirm the differential expression results obtained by the *microarray* experiments. Total RNA was extracted and purified using the experimental protocols described above. Total RNA (1 μg) was reverse-transcribed into cDNA, and then the cDNA samples were subjected to quantitative real time polymerase chain reaction (qRT-PCR) using a Applied Biosystems StepOneTM Real-Time PCR System (Life Technologies, Carlsbad, USA) Oligonucleotide *primer*s were designed for RPS18, PTGER2, IL1, ANGPT4, PDGFD, FGF2 (Table 5) using *Primer* Express Software 2.0 (Applied Biosystems, Foster City, USA). All real-time *primer*s were initially tested against standards and a standard curve was generated.

The optimized PCR conditions were: initial denaturation at 94°C for 10 minutes, followed by 40 cycles consisting of denaturation at 94°C for 15 seconds, annealing at 60°C for 1 minute and extension at 72°C for 45 seconds, with a final extension step at 72°C for 2 minutes. Negative control reactions with no template (deionized water) were also included in each run. For each gene, all samples were amplified simultaneously in duplicate in one assay run. Analysis of relative gene expression was performed using the $2^{-\Delta\Delta CT}$ method. RPS18 was used as a housekeeping gene to normalize expression data.

Table 5. *Primer*s used in the Real-time PCR.

Gene	*Primer*
RPS18	Forward: GTGATCCCCGAGAAGTTTCA Reverse: AATGGCAGTGATAGCGAAGG
PTGER2	Forward: GAACTGCGAGAGTCGTCAGTATCTC Reverse: CCCCGGCCGTGAACAT
IL1R1	Forward: AAGTGGAATGGGTCGGAAATT Reverse: TGAAGGGTGTTCCAAAAACTGA
ANGPT4	Forward: GGCATCTACTATCCGGTTCATCA Reverse: CATGCGTGTGCCATGCA
PDGFD	Forward: TATGCTCATTGGATGCCTTGTC Reverse: TGCTGCTATCGGGACACTTTT
FGF2	Forward: AAGGATCCCAAGCGGCTCTA Reverse: CGGCCGTCTGGATGGA

5.4 Statistical analysis

The normality of all variables distribution was verified using Shapiro–Wilk's W test. For morphometry analysis, comparisons among groups were performed using one-way analysis of variance (ANOVA), complemented by Tukey post-test analysis. STATISTICA version 7.0 (data analysis software system - StatSoft Inc.) was used to carry out the statistical analysis. Values of $p<0.05$ were considered statistically significant.

5.5 RESULTS

5.5.1 Histological analysis

An overview of the representative histological sections of all experimental groups is demonstrated in Figure 7. For CG, in the bone defect area, it was possible to observe blood clotting with fibrin and inflammatory cells 12 hours after the surgery (Figure 7A). At the same experimental period, for LG, the center of the defect presented blood

clotting. However, fibrin and inflammatory infiltrate, with polymorphonuclear cells (mainly represented by neutrophils) was observed in most of the injury area (Figure 7B).

After 36 hours, for CG, histological analysis demonstrated blood clotting and inflammatory infiltrate, including polymorphonuclear cells in the bone defect area (Figure 7C). At the same period, for LG, intense inflammatory process and some granulation tissue, mainly at the periphery of the defect, was observed (Figure 7D).

On day 3 after surgery, histological analyses of the CG revealed that inflammatory cells still could be observed, especially in the central region of the defect. Moreover, granulation tissue and immature newly formed bone surrounding the border was found in most of the injury area (Figure 7E). For LG, some inflammatory cells were still observed. Most of the defect was filled by granulation tissue and immature newly formed bone at the periphery (Figure 7F). After 5 days, animals of CG presented inflammatory infiltrate, granulation tissue and immature newly formed bone (Figure 7G). For LG, granulation tissue and bone ingrowth, with a more organized tissue organization was observed when compared to the CG ones (Figure 7H).

On day 7 after surgery, in CG, granulation tissue was present in almost all defect area. Some immature newly formed bone was seen at the peripheral area of the injury (Figure 7E). At the same period, histology assessment revealed an absence of inflammatory cells in LG. In addition, the bone defects were filled with newly formed bone. Areas of granulation tissue still could be observed (Figure 7F).

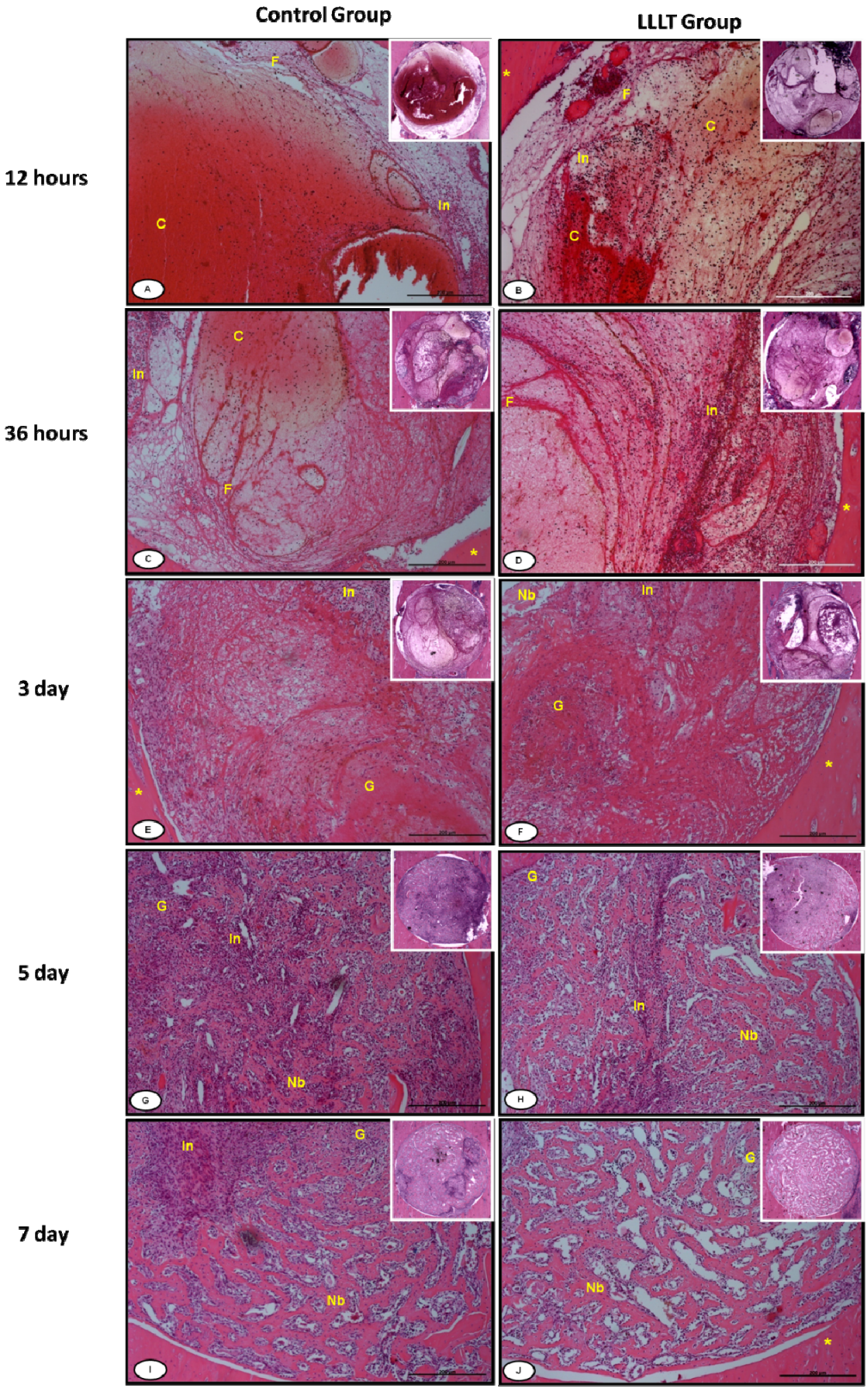

Figure 7. Overview and magnification of representative sections the control and laser irradiated groups showing newly formed bone (Nb), fibrin (F), granulation tissue (G), inflammatory infiltrate (In), blood clot (C). Hematoxylin and Eosin stain.

5.5.2 Morphometric analysis

Figure 8 shows the mean and standard deviation of the newly formed bone tissue area during the experimental periods. At 12 and 36 hours post-surgery, no newly formed bone was observed. Moreover, on days 3, 5 and 7 post-surgery, animals exposed to LLLT presented a statistically higher amount of newly formed bone when compared to the CG.

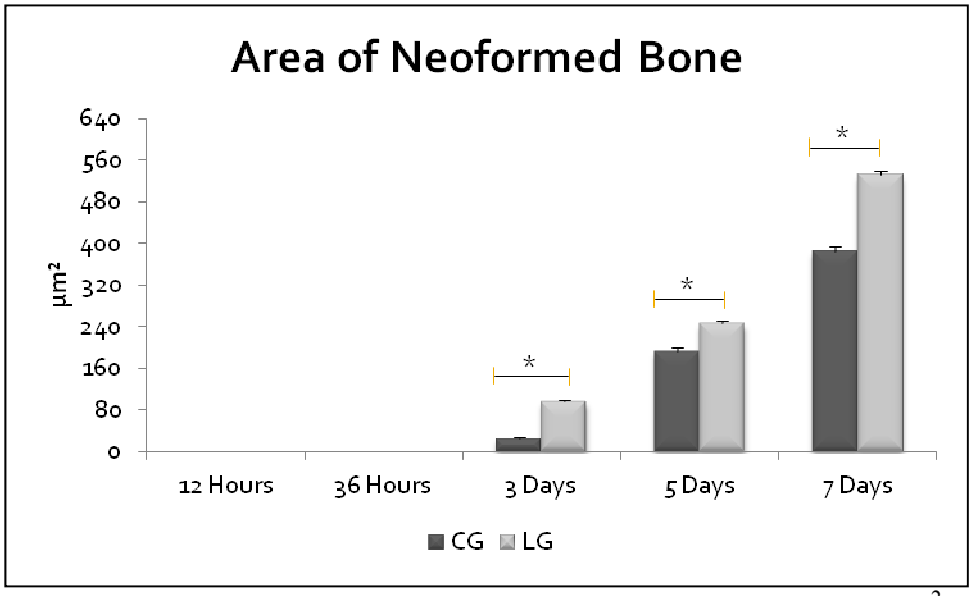

Figure 8. Means and SD of the newly formed bone tissue of bone area (μm^2) of the defect after treatments. Significant differences of $p < 0.001$ are represented by a single asterisk (*)

5.5.3 *Microarray* Analysis

By comparing the expression of genes between the reference time and LLLT treatment (12 h, 36 h, 3 d, 5 d and 7 d), a total of 10,837 genes modulated were identified after laser irradiation. The modulated genes have been organized in hierarchical cluster, which is shown in Figure 9.

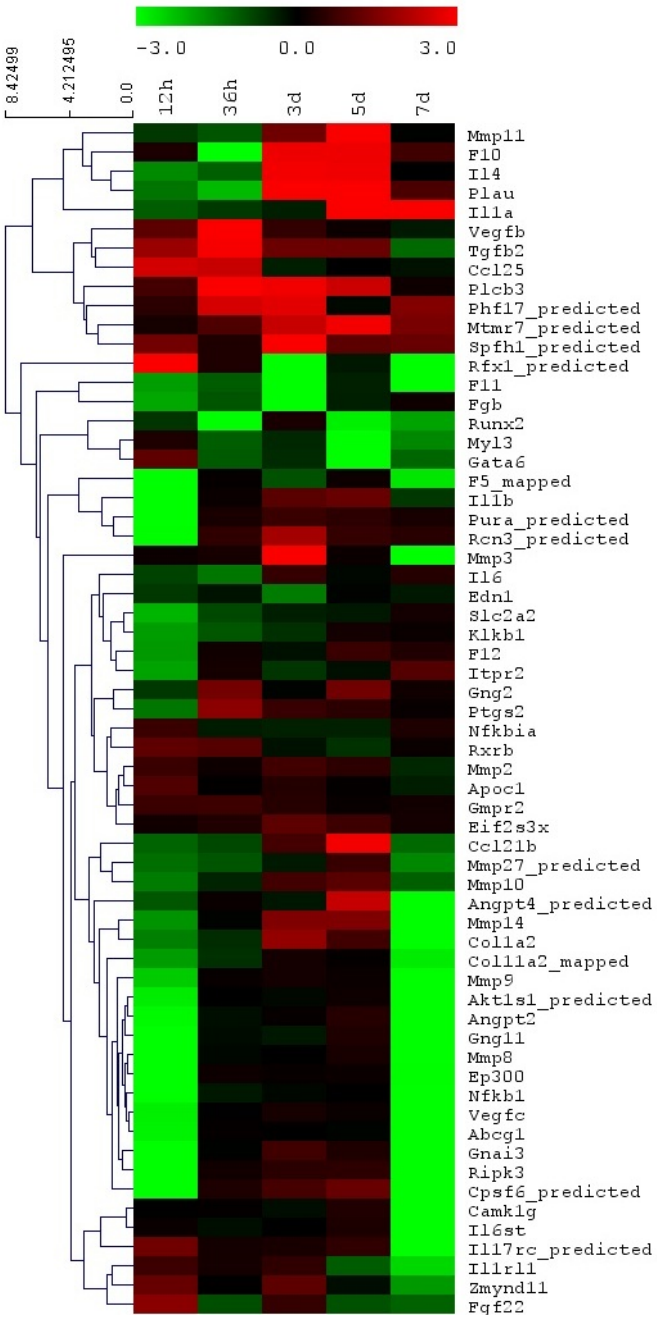

Figure 9. Hierarchical clustering showing the pattern of expression of genes during the Laser treatment. The color code display the $\log_2$ (Cy5/Cy3) ratio for each time point and has Cy3 as the reference value.

In order to try to refine the significance of the regulated genes in LG, the biological interactions using the IPA software tool were investigated. Thereby, several functional groupings of differentially expressed genes were identified, however this report focused on bone forming markers of early events of bone healing. Thus, the

osteogenic genes were examined and revealed that several genes up-regulation of TGF at 12 and 36 hours. Moreover, LLLT was efficient in stimulating the expression of BMP, FGF and RUNX-2 in all set points evaluated. In addition, OC was significantly up-regulated on day 3, 5 and 7. The altered expression of these genes suggests that LLLT acts on the stimulation of osteoblast and consequently in bone forming. The data concerning the up-regulation of osteogenic genes are demonstrated in table 6.

Table 6. List of the genes modulated after LLLT irradiation

Gene Symbol	Description	Fold Change
	12 hours	
BMP1	bone morphogenetic protein 1	1.083082
BMP2	bone morphogenetic protein 2	0.83399
BMP4	bone morphogenetic protein 4	0.98544
FGF4	fibroblast growth factor 4	2.347351
FGF22	fibroblast growth factor 22	1.179324
RUNX2	runt related transcription factor 2	1.201315
TGFb2	transforming growth factor, 2	1.107803
TGFbi	transforming growth factor, beta induced	1,162
	36 hours	
BMP3	bone morphogenetic protein 3	0.600393
BMP4	bone morphogenetic protein 4	0.655095
BMP7	bone morphogenetic protein 7	0.670662
FGF14	fibroblast growth factor 14	1.901222
FGF2	fibroblast growth factor 14	1.981114
RUNX2	runt related transcription factor 2	1.003231
TGFb1	transforming growth factor, beta 1	0.329877
TGFb2	transforming growth factor, beta 2	2.948775
TGFbi	transforming growth factor, beta induced	0.686692
	Day 3	
BMP2	bone morphogenetic protein 2	0.632143
RUNX2	runt related transcription factor 2	1.123382
OC	Osteocalcin	0.978488
FGF2	fibroblast growth factor 2	0.908738
FGF14	fibroblast growth factor 14	1.601722
	Day 5	
BMP3	bone morphogenetic protein 3	0.952591
FGF16	fibroblast growth factor 16	2.928107

FGF7	fibroblast growth factor 7	1.584963
FGF3	fibroblast growth factor 3	2.684498
FGF14	fibroblast growth factor 14	2.711495
OC	Osteocalcin	0.945301
RUNX2	runt related transcription factor 2	0.759818
	Day 7	
BMP2	bone morphogenetic protein 2	0.658781
BMP3	bone morphogenetic protein 3	1.059239
FGF14	fibroblast growth factor 14	0.568049
FGF3	fibroblast growth factor 3	3.6386
FGF4	fibroblast growth factor 4	0.599462
FGF2	fibroblast growth factor 2	0.808738
FGF15	fibroblast growth factor 15	0.546634
FGF5	fibroblast growth factor 5	0.568284
RUNX2	runt related transcription factor 2	0.959818
OC	Osteocalcin	0.926325

5.5.4 Validation of *microarray* data by real-time PCR

To validate the results of the *microarray* assays, we performed SYBR Green-based real-time PCR on control and irradiated group. We selected the genes according to the canonical pathway analysis and the references to previous studies. The expression profiles of the genes tested confirmed the *microarray* results.

5.6 DISCUSSION

This study aimed to evaluate the morphological changes induced by LLLT on the initial stages of bone healing and to study the pathways that stimulate the expression of genes related to bone cell proliferation and differentiation. The main findings showed that LLLT produced an earlier recruitment of inflammatory cells as well as a higher

amount of granulation tissue and increased the deposition of newly formed bone at the site of the injury. Also, it was evidenced that LLLT produced a significant increase in the expression of genes responsible for stimulating osteoblast proliferation and differentiation.

LLLT has been shown to have various biostimulatory effects, such as increase cell proliferation and accelerate tissue metabolism [12, 21, 22]. In this context, several studies demonstrated that LLLT had a positive effect in the process of bone consolidation in experimental models in rats [6, 23, 24]. These findings are in line with the results of the current study, which revealed that LLLT was able to modulate the inflammatory process in the area of the bone defect and to produce an earlier deposition of granulation tissue and newly formed bone. Moreover, LLLT increased the deposition of newly formed bone at the site of the injury. Our results suggest that LLLT stimulated osteoprogenitor cells and their differentiation into matrix-producing osteoblasts, thus increasing the rate of bone formation and bone ingrowth into the defect area observed in the LG.

In addition, *microarray* analysis demonstrated an up-regulation of TGF-β at 12 and 36 hours post-surgery in the LG, which may have contributed to stimulate the proliferation and differentiation of osteoblasts and consequently accelerated the process of bone healing. Specifically in bone healing, TGF-β is released by platelets in the initial inflammatory phase of fracture healing and may be involved in the initiation of callus formation [25]. In view of the aforementioned, it is possible to suggest that the increased amount of inflammatory infiltrate at 12 and 36 hours could be related to the up-regulation of TGF- β gene expression at these periods. Furthermore, TGF- β is the central player in bone homeostasis by inducing recruitment and proliferation of osteoblasts [25, 26] the up-regulation of this gene may have culminated in the

recruitment and proliferation of osteoblasts and consequently in the induction of newly formed bone. Similarly, Pyo *et al*., [27] demonstrated that LLLT induces gene expression of TGF-β1, BMP-2 and OC in 1% hypoxic cultured human osteoblasts.

Furthermore, it has been reported that TGF-β could induce BMP expression [28]. BMPs belong to the TGF-β superfamily and play an important role in embryonic development and bone formation [29]. To date, there are more than 20 known BMP subgroups of which, BMP- 2, 4, 5, 6, and 7 are thought to have the most important roles in the skeletal system [30, 31]. Other gene that is essential to induce osteogenesis is the RUNX-2 [32, 33]. RUNX2 is a member of the RUNX family and it is important for osteoblastic differentiation and skeletal morphogenesis and acts on regulatory factors involved in skeletal gene expression [34]. In this way, BMP and Runx2 serve as upstream and downstream "anchors" in the pathway that drives osteoblast differentiation [35]. In the present study, an increase in gene expression of BMP and RUNX-2, 12 and 36 hours and on day 3, 5 and 7 post-surgery was observed. These results are in agreement with those found by Fávaro-Pípi *et al*. [13], who demonstrated that LLLT was able of inducing a higher expression of mRNA of BMP4, phosphatase alkaline (ALP) and RUNX-2 at the site of the fracture in an experimental model of bone defect in the tibias of rats.

Furthermore, RUNX-2 stimulates osteoblast proliferation and induce the synthesis of collagen, OC, and other extracellular matrix proteins [36, 37]. OC is a marker of bone formation [38] and their expression in osteoblast cultures is used as a valid marker of osteoblast metabolic activity and mineral deposition [39]. Our *microarray* data also showed that LLLT produced an up-regulation of OC on days 3, 5 and 7 post surgery. These results suggest that LLLT stimulates the deposition of newly formed bone and accelerated tissue repair, as was demonstrated in histopathological

analysis. Similarly, Fernandes *et al*., [40] using an experimental model of tibial bone defect, showed that LLLT produced a significant increase in the expression of OC after three and five days. In addition, Stein *et al*. [41] observed an increase in OC mRNA expression in human osteoblastic cells, 72 h after LLLT application.

Bone development is also dependent on the expression of members of the FGF family expressed locally during bone formation [42]. There are 22 members of the FGF family. FGF-2 has been the most studied growth factor in bone, which is synthesized by osteoblasts/stromal cells and stored in the extracellular matrix [43]. In the present study, the expression of FGF was increased in all set points evaluated. These results are in agreement with Saygun *et al*., [45] who demonstrated that LLLT produced an increase in the proliferation of osteoblast cells and stimulated the release of bFGF, IGF-I, and IGFBP3 from these cells. As the rising of FGF stimulated the proliferation of various cell types including fibroblasts and osteoblasts [46] the up-regulation of this gene may indicate the presence of more active fibroblasts and osteoblasts, which could be related to the increase of granulation tissue and newly formed bone observed in the histological analysis in the LLLT group.

Taken together, the results of the present study suggest that LLLT might be promising to improve bone consolidation in the initial period of repair by modulating the expression of genes related to markers of bone formation and osteoblast activity, which may culminate in the stimulation of bone cells and increased newly formed bone.

5.7 CONCLUSION

In conclusion, the results found in the present study indicate that LLLT improved bone healing by producing a significant increase in the expression of osteogenic genes. Consequently, these data highlight the potential of the use of this therapy to improve the biological performance of bone regeneration applications. Further long-term studies should be carried out to provide additional information concerning the late stages of the interaction between LLLT and bone healing process.

Acknowledgments

We would like to acknowledge the contributions of Brazilian funding agency Fapesp (2010/15335-0) and the Center for Computational Engineering and Sciences at UNICAMP SP Brazil (FAPESP/CEPID and project #2013/08293-7) for the financial support of this research.

5.8 REFERENCES

1. Sella VR, do Bomfim FR, Machado PC, da Silva Morsoleto MJ, Chohfi M, Plapler H (2015) Effect of low-level laser therapy on bone repair: a randomized controlled experimental study. Lasers Med Sci. [Epub ahead of print].

2. Claes L, Willie B (2007) The enhancement of bone regeneration by ultrasound. Prog Biophys Mol Biol 93:384–398.

3. Einhorn TA, Gerstenfeld LC (2015) Fracture healing: mechanisms and interventions. Nat Rev Rheumatol 11(1):45-54.

4. Hoppe A, Güldal NS, Boccaccini AR (2011) A review of the biological response to ionic dissolution products from bioactive glasses and glass-ceramics. Biomaterials 32(11):2757-74.

5. Manteifel V, Bakeeva L, Karu T (1997) Ultrastructural changes in chondriome of human lymphocytes after irradiation with He-Ne laser: appearance of giant mitochondria. J Photochem Photobiol B 38:25-30.

6. Bossini PS, C, Ribeiro DA, Fangel R, C, Lahoz M De A, Parizotto NA (2012) Low level laser therapy (830nm) improves bone repair in osteoporotic rats: similar outcomes at two different dosages. Exp Gerontol 2:136-42.

7. Tim CR, Pinto KN, Rossi BR, Fernandes K, Matsumoto MA, Parizotto NA, Rennó AC (2014) Low-level laser therapy enhances the expression of osteogenic factors during bone repair in rats. Lasers Med Sci 1:147-56.

8. Oliveira P, Santos AA, Rodrigues T, Tim CR, Pinto KZ, Magri AM, Fernandes KR, Mattiello SM, Parizotto NA, Anibal FF, Rennó AC (2013) Effects of phototherapy on cartilage structure and inflammatory markers in an experimental model of osteoarthritis. J Biomed Opt. 18:128004.

9. Carrinho PM, Renno AC, Koeke P, Salate AC, Parizotto NA, Vidal BC (2006) Comparative study using 685-nm and 830-nm lasers in the tissue repair of tenotomized tendons in the mouse. Photomed Laser Surg 24:754-758.

10. Karu TI, Piatibrat LV, Kalendo GS (1999) Suppression of the intracellular concentration of ATP by irradiating with a laser pulse of wavelength lambda=820 nm. Dokl Akad Nauk 364:399-401.

11. Buravlev EA, Zhidkova TV, Osipov AN, Vladimirov YA (2015) Are the mitochondrial respiratory complexes blocked by NO the targets for the laser and LED therapy? Lasers Med Sci 30:173-80.

12. Stein A, Benayahu D, Maltz L, Oron U (2005) Low-level laser irradiation promotes proliferation and differentiation of human osteoblasts in vitro. Photomed Laser Surg 23:161-6.

13. Fávaro-Pípi E, Ribeiro DA, Ribeiro JU, Bossini P, Oliveira P, Parizotto NA, Tim C, de Araújo HS, Renno AC (2011) Low-level laser therapy induces differential expression of osteogenic genes during bone repair in rats. Photomed Laser Surg 29:311-7.

14. Wu YH, Wang J, Gong DX, Gu HY, Hu SS, Zhang H (2012) Effects of low-level laser irradiation on mesenchymal stem cell proliferation: a *microarray* analysis. Lasers Med Sci 27:509-519.

15. Laraia EM, Silva IS, Pereira DM, dos Reis FA, Albertini R, de Almeida P, Leal Junior EC, de Tarso Camillo de Carvalho P (2012) Effect of low-level laser therapy (660 nm) on acute inflammation induced by tenotomy of Achilles tendon in rats. Photochem Photobiol 88:1546–50.

16. de Lima FM, Villaverde AB, Albertini R, Corrêa JC, Carvalho RL, Munin E, Araújo T, Silva JA, Aimbire F (2011) Dual Effect of low-level laser therapy (LLLT) on the

acute lung inflammation induced by intestinal ischemia and reperfusion: action on anti- and pro-inflammatory cytokines. Lasers Surg Med 43:410–20.

17. Corazza AV, Jorge J, Kurachi C, Bagnato VS (2007) Photobiomodulation on the angiogenesis of skin wounds in rats using different light sources" Photomed. Laser Surg. 25:102-..

18. Assis L, Moretti AI, Abrahão TB, Cury V, Souza HP, Hamblin MR, Parizotto NA (2012) Low-level laser therapy (808 nm) reduces inflammatory response and oxidative stress in rat tibialis anterior muscle after cryolesion," Lasers Surg Med 44:726-35.

19. da Silva AP, Petri AD, Crippa GE, Stuani AS, Stuani AS, Rosa AL, Stuani MB (2012) Effect of low-level laser therapy after rapid maxillary expansion on proliferation and differentiation of osteoblastic cells. Lasers Med Sci 27:777-83.

20. de Castro PA, Savoldi M, Bonatto D, Malavazi I, Goldman MH, Berretta AA, Goldman GH (2012) Transcriptional profiling of Saccharomyces cerevisiae exposed to propolis," BMC Complement Altern Med 24, 194.

21. Soleimani M, Abbasnia E, Fathi M, Sahraei H, Fathi Y, Kaka G (2012) The effects of low-level laser irradiation on differentiation and proliferation of human bone marrow mesenchymal stem cells into neurons and osteoblasts--an in vitro study. Lasers Med Sci 27:423-30.

22. Medina-Huertas R, Manzano-Moreno FJ, De Luna-Bertos E, Ramos-Torrecillas J, García-Martínez O, Ruiz C The effects of low-level diode laser irradiation on differentiation, antigenic profile, and phagocytic capacity of osteoblast-like cells (MG-63). Lasers Med Sci 29:1479-84.

23. Matsumoto MA, Ferino FV, Monteleone GF, Ribeiro DA (2009) Low level laser therapy modulates cyclo-oxygenase-2 expression during boné repair in rats. Lasers Med Sci 24:196-201.

24. Altan AB, Bicakci AA, Avunduk MC, Esen H (2015) The effect of dosage on the efficiency of LLLT in new bone formation at the expanded suture in rats. Lasers Med Sci 30:255-62.

25. Kulterer B, Friedl G, Jandrositz A, Sanchez-Cabo F, Prokesch A, Paar C, Scheideler M, Windhager R, Preisegger KH, Trajanoski Z (2007) Gene expression profiling of human mesenchymal stem cells derived from bone marrow during expansion and osteoblast differentiation. BMC Genomics 12;8:70.

26. Li WG, Xu XX (2005) The expression of N-cadherin, fibronectin during chondrogenic differentiation of MSC induced by TGF-beta(1). Chin J Traumatol 8:349-351.

27. Pyo SJ, Song WW, Kim IR, Park BS, Kim CH, Shin SH, Chung IK, Kim YD (2013) Low-level laser therapy induces the expressions of BMP-2, osteocalcin, and TGF-β1 in hypoxic-cultured human osteoblasts. Lasers Med Sci 2:543-50.

28. Chen MH, Huang YC, Sun JS, Chao YH, Chen MH (2014) Second messengers mediating the proliferation and collagen synthesis of tenocytes induced by low-level laser irradiation. Lasers Med Sci 30:263-72.

29. Bessa PC, Casal M, Reis RL (2008) Bone morphogenetic proteins in tissue engineering: the road from the laboratory to the clinic, part I (basic concepts). J Tissue Eng Regen Med 2:1-13.

30. Reddi AH (2001) Bone morphogenetic proteins: From basic science to clinical applications. J Bone Joint Surg 83-A:S1–S6.

31. Kloen P, Di Paola M, Borens O, Richmond J, Perino G, Helfet DL, Goumans MJ (2003) BMP signaling components are expressed in human fracture callus. Bone 33:362–371.

32. Ducy P (2000) Cbfa1: A molecular switch in osteoblast biology. Dev. Dyn. 219: 461–471.

33. Canalis E, Economides AN, Gazzerro E (2003) Bone morphogenetic proteins, their antagonists, and the skeleton. Endocr. Rev. 24: 218–235.

34. McGee-Lawrence ME, Li X, Bledsoe KL, Wu H, Hawse JR, Subramaniam M, Razidlo DF, Stensgard BA, Stein GS, van Wijnen AJ, Lian JB, Hsu W, Westendorf JJ (2013) Runx2 protein repress Axin2 expression in osteoblasts and is required for cranio synostosis in Axin2-deficient mice. J Biol Chem 288: 5291-302.

35. Derynck R, Miyazono K (2008) The TGF-β Family Cold Spring Harbor Laboratory Press.

36. Komori T (2006) Regulation of osteoblast differentiation by transcription factors. J Cell Biochem 99:1233–1239

37. Mendelson A, Frank E, Allred C, Jones E, Chen M, Zhao W, Mao JJ (2011) Chondrogenesis by chemotactic homing of synovium, bone marrow, and adipose stem cells in vitro. FASEB J 25:3496–3504.

38. Bar I, Zilberman Y, Zeira E, Galun E, Honigman A, Turgeman G, Clemens T, Gazit Z, Gazit D (2003) Molecular imaging of the skeleton: quantitative real-time bioluminescence monitoring gene expression in bone repair and development. J Bone Miner Res 18:570-8.

39. Cantatore FP, Corrado A, Grano M, Quarta L, Colucci S, Melillo N (2004) Osteocalcin synthesis by human osteoblasts from normal and osteoarthritic bone after vitamin D3 stimulation. Clin Rheumatol 23:490-5.

40. Fernandes KR, Ribeiro DA, Rodrigues NC, Tim C, Santos AA, Parizotto NA, De Araujo HS, Driusso P, Rennó AC (2013) Effects of low-level laser therapy on the expression of osteogenic genes related in the initial stages of bone defects in rats. J Biomed Opt 3:038002.

41. Stein E, Koehn J, Sutter W, Wendtlandt G, Wanschitz F, Thurnher D, Baghestanian M, Turhani D (2008) Initial effects of low-level laser therapy on growth and differentiation of human osteoblast-like cells. Initial effects of low-level laser therapy on growth and differentiation of human osteoblast-like cells. Wien Klin Wochenschr 120:112-7.

42. Marie PJ (2003) Fibroblast growth factor signaling controlling osteoblast differentiation. Gene 316: 23–32.

43. Boden SD (2005) The ABCs of BMPs. Orthop Nurs 24:49-52.

44. Saygun I, Nizam N, Ural AU, Serdar MA, Avcu F, Tözüm TF (2012) Low-Level Laser Irradiation Affects the Release of Basic Fibroblast Growth Factor (bFGF), Insulin-Like Growth Factor-I (IGF-I), and Receptor of IGF-I (IGFBP3) from Osteoblasts. Photomedicine and Laser Surgery 30:149-54.

45. Du X, Xie Y, Xian CJ, Chen L (2012) Role of FGFs/FGFRs in skeletal development and bone regeneration. J Cell Physiol 227:3731-3743.

Parte III

---

6. CONSIDERAÇÕES FINAIS E PERSPECTIVAS FUTURAS

7. REFERÊNCIAS

8. ANEXOS

6. CONSIDERAÇÕES FINAIS E PERSPECTIVAS FUTURAS

Em síntese, pode-se concluir que a LLLT induziu a resolução da inflamação através da modulação de genes envolvidos neste processo, foi eficaz na estimulação da angiogenese na fase inicial de reparo e ainda, produziu aumento de genes osteogênicos que podem ter estimulado a diferenciação e proliferação de osteoblastos, que consequentemente podem ser relacionados com a deposição de tecido ósseo neoformado observado na área da lesão.

A respeito das perspectivas futuras, mais estudos são oportunos para melhor elucidar esta questão, principalmente envolvendo estudos investigando defeitos ósseos considerados de tamanho crítico e estudos longitudinais do tratamento Laser para verificar a sua influência sobre a expressão gênica global.

7. REFERÊNCIAS

AGAS, D.; SABBIETI, M.G.; MARCHETTI, L.; XIAO, L.; HURLEY, M.M. FGF-2 enhances Runx-2/Smads nuclear localization in BMP-2 canonical signaling in osteoblasts. **J Cell Physiol**, 11:2149-58, 2013.

ALEKSIC, V.; AOKI, A.; IWASAKI, K.; TAKASAKI, A.A.; WANG, C.Y.; ABIKO, Y.; ISHIKAWA, I.; IZUMI, Y. Low-level Er:YAG laser irradiation enhances osteoblast proliferation through activation of MAPK/ERK. **Lasers Med Sci,** 4:559-69, 2010;25.

ANGELETTI, P.; PEREIRA, M.D.; GOMES, H.C.; HINO, C.T.; FERREIRA, L.M. Effect of low-level laser therapy (GaAlAs) on bone regeneration in midpalatal anterior suture after surgically assisted rapid maxillary expansion. **Oral Surg Oral Med Oral Pathol Oral Radiol Endod,** 3:e38-46, 2010.

BARUSHKA, O.; YAAKOBI, T.; ORON, U. Effect of low-energy laser (He-Ne) irradiation on the process of bone repair in the rat tibia. **Bone**, 16:47-55, 1995.

BAXTER GD. **Therapeutic lasers: theory and practice**. United States of America: Ed. Churchill Livingstone, 1-19, 1997.

BOSSINI, P.S.; FANGEL, R.; HABENSCHUS, R.M.; RENNO, A.C.; BENZE, B.; ZUANON, J.A.; NETO, C.B.; PARIZOTTO, N.A. Low-level laser therapy (670 nm) on viability of random skin flap in rats. **Lasers Med Sci.** 24:209-213, 2009.

BOSSINI, P.S.; RENNÓ, A.C.; RIBEIRO, D.A.; FANGEL, R.; RIBEIRO, A.C.; LAHOZ, M.; DE A.; PARIZOTTO, N.A. Low level laser therapy (830nm) improves bone repair in osteoporotic rats: similar outcomes at two different dosages. **Exp Gerontol**, 2:136-42, 2012.

BOUVET-GERBETTAZ, S.; MERIGO, E.; ROCCA, J.P.; CARLE, G.P.; ROCHET, N. Effects of low level laser therapy on proliferation and differentiation of murine boné marrow cells into osteoblasts and osteclasts. **Lasers Surg Med**, 41:291-297, 2009.

BUCKWALTER, J.A.; EINHORN. T.A.; O'KEEFE R.J. **American Academy of Orthopaedic Surgeons Orthopaedic basic science: foundations of clinical practice.** 3° edition: Rosemont, American Academy of Orthopaedic Surgeons, 2007.

CANALIS, E.; ECONOMIDES, A. N. ; GAZZERRO, E. Bone Morphogenetic Proteins, Their Antagonists, and the Skeleton. **Endocrine Reviews,** 2:218–235, 2003.

CEPERA, F.; TORRES, F.C.; SCANAVINI, M.A.; PARANHOS, L.R.; CAPELOZZA FILHO, L.; CARDOSO, M.A.; SIQUEIRA, D.C.; SIQUEIRA, D.F. Effect of a low-

level laser on bone regeneration after rapid maxillary expansion. Am J Orthod Dentofacial Orthop. 141:444-50. 2012.

CHANG, J.L.; BRAUER, D.S.; JOHNSON, J.; CHEN, C.G.; AKIL, O.; BALOOCH, G.; HUMPHREY, M.B.; CHIN, EN.; PORTER, A.E.; BUTCHER, K.; RITCHIE, R.O.; SCHNEIDER, R.A.; LALWANI, A.; DERYNCK, R.; MARSHALL, G.W.; MARSHALL, S.J.; LUSTIG, L.; ALLISTON, T. Tissue-specific calibration of extracellular matrix material properties by transforming growth factor-β and runx2 in bone is required for hearing. **EMBO REP,** 10:765-71, 2010.

CLAES, L; WILLIE , B. The enhancement of bone regeneration by ultrasound. **Prog Biophys Mol Biol**, 93:384–398, 2007.

DORTBUDAK, O.; HAAS, R.; MALLATH-POKORNY, G. Biostimulation of bone marrow cells with a diode soft laser. **Clin Oral Implants Res,** 2000; 11: 540-545.

ECKARDT, H.; DING, M.; LIND, M.; HANSEN, E.S.; CHRISTENSEN, K.S.; HVID, I. Recombinant human vascular endothelial growth factor enhances bone healing in an experimental nonunion model. **J Bone Joint Surg Br**, 10:1434-8, 2005.

FERNANDES, K.R.; RIBEIRO, D.A.; RODRIGUES, N.C.; TIM, C.; SANTOS, A.A.; PARIZOTTO, N.A.; DE ARAUJO H.S.; DRIUSSO, P.; RENNÓ, A.C. Effects of low-level laser therapy on the expression of osteogenic genes related in the initial stages of bone defects in rats. **J Biomed Opt**, 3:038002, 2013.

GUARTNER, L. P.; HIATT, J. L. **Tratado de histologia**. 2ed. Rio de Janeiro: Guanabara Koogan, 2003.

HADJIARGYROU, M.; KENNETH, M.; RYABY, J.P.; RUBIN, C. Enhancement of frature healing by low intensity ultrasound. **Clin Orthop Relat Res,** 355:216-229, 1998.

HANKENSON, K.D.; DISHOWITZ, M.; GRAY, C.; SCHENKER, M. Angiogenesis in bone regeneration. **Injury**, 6:556-61, 2011.

HING K.A. Bone repair in the twenty-first century: biology, chemistry or engineering? **Philos Trans A Math Phys Eng Sci**, 1825:2821-50, 2004.

KARU, T.I.; KOLYAKOV, S.F. Exact action spectra of cellular responses relevant to phototherapy. **Photomed Laser Surg**, 23:356-361, 2005.

KAYAL, R.A.; ALBLOWI, J.; MCKENZIE, E.; KROTHAPALLI, N.; SILKMAN, L.; GERSTENFELD, L.; EINHORN, T.A. GRAVES, D.T. Diabetes causes the accelerated loss of cartilage during fracture repair which is reserved by insulin treatment. **Bone,** 44:357-363, 2009.

KERA MARIS, N.C.; CALORI, G.M.; NIKOLAOU, V.S. Fracture vascularity and bone healing: a systematic review of the role of VEGF. **Injury**, 2:S45–57, 2008.

KLOTING, N.; FOLLAK, N.; KLOTING, I. Is there an autoimmune process in bone? Gene expression studies in diabetic and nondiabetic BB rat as well as BB rat-related andunrelated rat strains. **Physiol Genomics**, 24:59-64, 2005.

LEHMANN, W.; EDGAR, C.M.; WANG, K. Tumor necrosis factor alpha (TNF-alpha) coordinately regulates the expression of specific matrix metalloproteinases (MMPS) and angiogenic factors during fracture healing. **Bone**, 2: 300–10, 2005.

LIRANI-GALVÃO, A.P.; JORGETTI, V.; DA SILVA, O.L. Comparative study of how low-level laser therapy and low-intensity pulsed ultrasound affect bone repair in rats. **Photomed Laser Surg**, 24:735-740, 2006.

LU, C.; MARCUCIO, R.; MICLAU, T. Assessing angiogenesis during fracture healing. **Iowa Orthop J**, 26:17-26, 2006.

MARSELL, R.; EINHORN, T.A. Emerging bone healing therapies. **J Orthop Trauma,** 24(1):S4–8, 2010.

NINOMIYA, T.; HOSOYA, A.; NAKAMURA, H.; SANO, K.; NISHISAKA, T.; OZAWA H. Increase of bone volume by a nanosecond pulsed laser irradiation is caused by a decreased osteoclast number and an activated osteoblast. **Bone,** 40:140-148, 2007.

OLIVEIRA, P.; RIBEIRO, D.A.; FAVARO-PIPI, E.; DRIUSSO, P.; PARIZOTTO, N.A.; RENNO, A.C.M. Low level laser therapy does not modulate the outcomes of a highly bioactive glass–ceramic (Biosilicate®) on bone consolidation in rats. **J Mater Sci: Mater Med**., 2009.

ORTIZ, M.C.S.; CARRINHO, P.M.; DOS SANTOS, A.A.S.; GOLÇALVES, R.C.; PARIZOTTO, N.A. Laser de baixa intensidade: princípios e generalidades – Parte 1. **Fisioterapia Brasil**, 2: 221-236, 2001.

ORYAN, A.; MONAZZAH, S.; BIGHAM-SADEGH, A. Bone Injury and Fracture Healing Biology. **Biomed Environ Sci.** 28:57-71, 2015.

OZAWA, Y.; SHIMIZU, N.; KARIYA, G.; ABIKO, Y. Low-energy laser irradiation stimulates bone nodule formation at early stages of cell culture in rat calvarial cells. **Bone**, 22:347-354, 1998.

PACICCA, D.M.; PATEL, N.; LEE, C.; SALISBURY, K.; LEHMANN, W.; CARVALHO, R.; GERSTENFELD, L.C.; EINHORN, T.A. Expression of angiogenic factors during distraction osteogenesis. **Bone**, 33: 889–898, 2003.

PATROCÍNIO-SILVA, T.L.; DE SOUZA, A.M.; GOULART, R.L.; PEGORARI, C.F.; OLIVEIRA, J.R.; FERNANDES, K.; MAGRI, A.; PEREIRA, R.M.; ARAKI, D.R.;

NAGAOKA, M.R.; PARIZOTTO, N.A.; RENNÓ, A.C. The effects of low-level laser irradiation on bone tissue in diabetic rats. **Lasers Med Sci.** 29:1357-64, 2014.

PHILLIPS, A.M. Overview of the fracture healing cascade. **Injury,** 2005.

PINHEIRO, A.L.B.; OLIVEIRA, G.M.; MARTINS, P.P.M.; RAMALHO, L.M.P.; OLIVEIRA, M.A.M.; JÚNIOR, N.A.; NICOLAU, R.M. Biomodulatory effects of LLLT on bone regeneration. **Laser Therapy,** 13:73-79, 2001.

PYO, S.J.; SONG, W.W.; KIM, I.R.; PARK, B.S.; KIM, C.H.; SHIN, S.H.; CHUNG, I.K.; KIM, Y.D. Low-level laser therapy induces the expressions of BMP-2, osteocalcin, and TGF-β1 in hypoxic-cultured human osteoblasts. **Lasers Med Sci.** 2:543-50, 2013.

RATH, B.; NAM, J.; KNOBLOCH, T.J.; LANNUTTI, J.J.; AGARWALL, S. Compressive forces induce osteogenic gene expression in calvarial osteoblasts. **J Biomech**. 41:1095-1103, 2008.

RENNO, A.C.M.; McDONNELL, P.A.; PARIZOTTO, N.A.; LAAKSO, E-L. The effects of laser irradiation on osteoblast and osteosarcoma cell proliferation and differentiation *in vitro*. **Photomed Laser Surg**, 25:275-80, 2007.

RODRIGUES, N.C.; BRUNELLI, R.; DE ARAÚJO, H.S.; PARIZOTTO, N.A.; RENNO, A.C. Low-level laser therapy (LLLT) (660nm) alters gene expression during muscle healing in rats. J **Photochem Photobiol B**,120: 29-35, 2013.

SCHINDELER, A.; MCDONALD, M.M.; BOKKO, P.; LITTLE, D.G. Bone remodeling during fracture repair: The cellular Picture. **Semin Cell Dev Biol,** 19:459-466, 2008.

SELLA, V.R; DO BOMFIM, F.R.; MACHADO, P.C.; DA SILVA MORSOLETO, M.J.; CHOHFI, M.; PLAPLER, H. Effect of low-level laser therapy on bone repair: a randomized controlled experimental study. Lasers Med Sci, 2015 [Epub ahead of print].

SENA, K.; LEVEN, R.M.; MAZHAR, K.; SUMMER, D.R.; VIRDI, A.S. Early gene response to low intensity pulsed ultrasound in rat osteoblastic cells. **Ultrasound Med Biol,** 31:703-708, 2005.

SILVA, R.V. ;CAMILLI, J.A. Repair of Bone Defects Treated with Autogenous Bone Graft and Low-Power Laser. **J CranioFac Surg,** 2006.

SONG, S.L.; HUTMACHER, D.; NURCOMBE, V.; COOL, S.M. Temporal expression of proteoglycans in the rat limb during bone healing. **Gene**, 379: 92-100, 2006.

STEIN, E.; KOEHN, J.; SUTTER, W.; WENDTLANDT, G.; WANSCHITZ, F.; THURNHER, D.; BAGHESTANIAN, M.; TURHANI, D. Initial effects of low-level

laser therapy on growth and differentiation of human osteoblast-like cells. **Wien Klin Wochenschr.**, 120:112-117, 2008.

TIM, C.R.; PINTO, K.N.; ROSSI, B.R.; FERNANDES, K.; MATSUMOTO, M.A.; PARIZOTTO, N.A.; RENNÓ, A.C. Low-level laser therapy enhances the expression of osteogenic factors during bone repair in rats. **Lasers Med Sci.** 1:147-56, 2014.

TSIRIDIS, E.; UPADHYAY, N.; GIANNOUDIS, P. Molecular aspects of fracture healing: which are the important molecules? **Injury**, (1):S11–25, 2007.

YAOITA, H.; ORIMO, H.; HHIRAI, Y.; SHIMADA, T. Expression of bone morphogenetic proteins and rat distal-less homolog genes following rat femoral fracture. **J Bone Miner Metab,** 18:63-70, 2000.

ZHANG, X.; SCHWARZ, E.M.; YOUNG, D.A.; PUZAS, E.; ROSIER, R.N.; O'KEEFE, R.J. Cyclo-oxygenase-2 regulates mesenchymal cell differentiation into the osteoblast lineage and is critically involved in bone repair. **J Clin Invest.** v.109, p.1405-1415, 2002.

ZIROS, P.G.; BASDRA, E.K.; PAPAVASSILIOU, A.G. Runx-2: of bone and stretch. **Int J Biochem Cell Biol**. 40:1659-1663, 2008.

Anexo A: Parecer do Comissão de Ética no Uso de Animais

UNIVERSIDADE FEDERAL DE SÃO CARLOS
PRÓ-REITORIA DE PESQUISA
Comissão de Ética no Uso de Animais
Via Washington Luís, km. 235 - Caixa Postal 676
Fones: (016) 3351.8109 / 3351.8110
Fax: (016) 3361.3176
CEP 13560-970 - São Carlos - SP - Brasil
ceua@ufscar.br - www.propq.ufscar.br

Parecer da Comissão de Ética no Uso de Animais

nº 026/2011

Protocolo nº. 010/2011

A Comissão de Ética no Uso de Animais da Universidade Federal de São Carlos - CEUA/UFSCar **APROVOU** o projeto sob título ***"Análise da expressão gênica durante o reparo ósseo em defeitos de tíbias iradiadas com laser terapêutico de baixa intensidade"*** elaborado pela pesquisadora Carla Roberta Tim.

São Carlos, 29 de junho de 2011.

Profa. Dra. Luciana Thie Seki Dias
Presidente da Comissão de Ética no Uso de Animais